International Journal of Heat and Mass Transfer 64 (2013) 1239–1256

Contents lists available at SciVerse ScienceDirect

International Journal of Heat and Mass Transfer

journal homepage: www.elsevier.com/locate/ijhmt

Universal approach to predicting saturated flow boiling heat transfer in mini/micro-channels – Part II. Two-phase heat transfer coefficient

Sung-Min Kim, Issam Mudawar *

Boiling and Two-Phase Flow Laboratory (BTPFL) and Purdue University International Electronic Cooling Alliance (PUIECA), Mechanical Engineering Building, 585 Purdue Mall, West Lafayette, IN 47907-2088, USA

ARTICLE INFO

Article history:
Available online 9 May 2013

Keywords:
Heat transfer coefficient
Dryout incipience
Flow boiling
Mini-channel
Micro-channel

ABSTRACT

This second part of a two-part study examines the prediction of saturated flow boiling heat transfer in mini/micro-channels. The first part culminated in a technique for determining the dryout incipience quality corresponding to substantial deterioration in the heat transfer coefficient. In this part, a consolidated database for flow boiling in mini/micro-channels is amassed from 31 sources, of which 10,805 data points are designated as pre-dryout. The pre-dryout database consists of 18 working fluids, hydraulic diameters of 0.19–6.5 mm, mass velocities of 19–1608 $kg/m^2 s$, liquid-only Reynolds numbers of 57–49,820, qualities of 0–1, and reduced pressures of 0.005–0.69. The pre-dryout database is used to evaluate prior correlations that have been recommended for both macro-channels and mini/micro-channels. A few of these correlations are shown to provide fair overall performance, but their accuracy is compromised against specific portions of the database, especially high pressures and very small diameters. A new generalized correlation is constructed by superpositioning the contributions of nucleate boiling and convective boiling. This correlation is shown to provide very good predictions against the entire pre-dryout database, evidenced by an overall MAE of 20.3%, with 79.9% and 95.5% of the data falling within ±30% and ±50% error bands, respectively. Evenly good predictions are achieved for all working fluids and all ranges of the database parameters.

© 2013 Elsevier Ltd. All rights reserved.

1. Introduction

Two-phase mini/micro-channel devices have gained unprecedented popularity in recent years in many applications demanding the dissipation of large amounts of heat from very small areas [1–3]. While other two-phase cooling schemes, including pool boiling [4,5], jet [6–9] and spray [10–13], and surface enhancement [14–16], have also been considered for similar applications, two-phase mini/micro-channel devices have been favored for their compactness, relative ease of fabrication, high heat dissipation to volume ratio, and small coolant inventory. They have also shown remarkable adaptability for implementation into hybrid cooling schemes that combine the benefits of mini/micro-channels with those of jet impingement [17,18].

The immense interest in two-phase mini/micro-channel cooling has spurred an unusually large number of articles during the past few years, with special attention paid to the prediction of pressure drop and heat transfer characteristics. Unfortunately, the large number of articles has inadvertently led to tremendous confusion in the use of thermal design tools. Therefore, there is now an urgent need to (i) evaluate the large body of literature concerning flow boiling in small channels, and (ii) consolidate published findings into 'universal' predictive tools that are applicable to numerous working fluids and broad ranges of operating conditions.

This need has been the primary motivation for a series of studies that have been recently pursued at the Purdue University Boiling and Two-Phase Flow Laboratory (PU-BTPFL) based on a methodology that was adopted earlier to predict critical heat flux (CHF) for water flow in tubes [19–21]. These efforts involved consolidation of published databases for mini/micro-channels, and development of universal predictive tools for pressure drop [22,23] and condensation heat transfer coefficient [24].

The present two-part study continues these efforts by developing universal predictive tools for flow boiling heat transfer in mini/micro-channel. The first part of the study [25] explored dryout limits that constitute important boundaries to flow boiling heat transfer in small channels. Dryout is closely associated with the annular flow regime prevalent in saturated flow boiling in mini/micro-channels. However, the axial span of annular flow is highly dependent on working fluid and operating conditions. Two distinct heat transfer regimes have been identified based on mechanisms that dominate the largest fraction of channel length upstream of the

* Corresponding author. Tel.: +1 765 494 5705; fax: +1 765 494 0539.
E-mail address: mudawar@ecn.purdue.edu (I. Mudawar).
URL: https://engineering.purdue.edu/BTPFL (I. Mudawar).

0017-9310/$ - see front matter © 2013 Elsevier Ltd. All rights reserved.
http://dx.doi.org/10.1016/j.ijheatmasstransfer.2013.04.014

Nomenclature

Bd	Bond number
Bo	Boiling number, q''_H/Gh_{fg}
C_1–C_5	empirical coefficients
Ca	Capillary number
Co	Convection number
D	tube diameter
D_h	hydraulic diameter
E	empirical coefficient
e	surface roughness
F	empirical coefficient
Fr	Froude number
G	mass velocity
g	gravitational acceleration
h	heat transfer coefficient
h_{fg}	latent heat of vaporization
h_{tp}	two-phase heat transfer coefficient
k	thermal conductivity
L	channel length
M	molecular weight
MAE	mean absolute error
N	number of data points; empirical coefficient
N_1–N_8	empirical exponents
N_{conf}	Confinement number
Nu	Nusselt number
P	pressure
P_{crit}	critical pressure
P_F	wetted perimeter of channel
P_H	heated perimeter of channel
P_R	reduced pressure, $P_R = P/P_{crit}$
Pr	Prandtl number
q''	heat flux
q''_H	heat flux based on heated perimeter of channel
Re	Reynolds number
Re_f	superficial liquid Reynolds number, $Re_f = G(1-x)D_h/\mu_f$
Re_{fo}	liquid-only Reynolds number, $Re_{fo} = GD_h/\mu_f$
Re_{go}	vapor-only Reynolds number, $Re_{go} = GD_h/\mu_g$
S	empirical coefficient
T	temperature
We	Weber number
x	thermodynamic equilibrium quality
x_{di}	dryout incipience quality
X_{tt}	Lockhart–Martinelli parameter based on turbulent liquid-turbulent vapor flows
z	stream-wise coordinate

Greek symbols

β	channel aspect ratio ($\beta < 1$)
θ	percentage predicted within ±30%
μ	dynamic viscosity
ξ	percentage predicted within ±50%
ρ	density
σ	surface tension

Subscripts

3	based on three-sided heat transfer in rectangular channel
4	based on four-sided heat transfer in rectangular channel
avg	average
cb	convective boiling dominant heat transfer
cir	based on uniform circumferential heating
Cooper	Cooper's correlation [64]
exp	experimental (measured)
f	saturated liquid
fo	liquid only
g	saturated vapor
go	vapor only
nb	nucleate boiling dominant heat transfer
pred	predicted
sat	saturation
sp	single-phase
tp	two-phase

dryout location. Shown in Fig. 1(a) is *Nucleate Boiling Dominant* heat transfer (*e.g.* [26–28]), where a significant fraction of the channel length is dominated by bubbly and slug flow, and the heat transfer coefficient decreases monotonically due to gradual suppression of nucleate boiling. Fig. 1(b) shows the second, *Convective Boiling Dominant* heat transfer (*e.g.* [29–31]), where a significant fraction of the channel length is dominated by annular flow, and the heat transfer coefficient increases along the channel due to gradual thinning of the annular liquid film. Dryout of the annular film constitutes an important operational limit for both heat transfer types. But because of a lack of symmetry in the formation and consumption of the annular film, initial dry patches begin to form at the location of *Dryout Incipience*, which marks the point of substantial reduction in the heat transfer. *Dryout Completion*, on the other hand, where the film is fully consumed, is encountered farther downstream.

With the dryout incipience accurately characterized in the first part of this study [25], the present part concerns the development of a generalized correlation for the pre-dryout two-phase heat transfer coefficient associated with saturated flow boiling in mini/micro-channels. To achieve this goal, published saturated flow boiling heat transfer databases for mini/micro-channel flows are amassed from 37 sources [26–62]. The newly consolidated database is then compared to predictions of previous correlations for both macro-channels [63–66] and mini/micro-channels [58,67–74]. A new generalized correlation technique is proposed, and its predictive accuracy validated for various working fluids and over very broad ranges of operating conditions.

2. New consolidated mini/micro-channel database

In the first part of the study [25], a generalized correlation for dryout incipience quality in was developed using five dimensionless parameters: Weber number, Capillary number, Boiling number, reduced pressure, and density ratio. Summarized in Table 1, the dryout incipience quality correlation was validated against a 997 point consolidated database for mini/micro-channels amassed from 26 sources with very good accuracy.

A new consolidated database consisting of 12,974 data points for flow boiling heat transfer in mini/micro-channels is amassed from 37 sources [26–62]. The database includes 11,409 single-channel data points from 31 sources, and 1565 multi-channel data points from 6 sources. To develop a generalized correlation for saturated flow boiling heat transfer (*i.e.*, pre-dryout heat transfer), 10,805 pre-dryout data points of the 12,974 point consolidated database are identified using the dryout incipience quality correlation in Table 1. Table 2 provides key information on the individual databases incorporated in the consolidated database in chronological order, along with the number of pre-dryout data points. Also

Table 1
Kim and Mudawar's [25] correlation for dryout incipience quality for saturated flow boiling in mini/micro-channels.

$x_{di} = 1.4We_{fo}^{0.03}P_R^{0.08} - 15.0\left(Bo\frac{P_H}{P_F}\right)^{0.15}Ca^{0.35}\left(\frac{\rho_g}{\rho_f}\right)^{0.06}$
where $We_{fo} = \frac{G^2D_h}{\rho_f\sigma}$, $P_R = \frac{P}{P_{crit}}$, $Bo = \frac{q''_H}{Gh_{fg}}$, $Ca = \frac{\mu_f G}{\rho_f\sigma}\left(=\frac{We_{fo}}{Re_{fo}}\right)$,
q''_H: effective heat flux averaged over heated perimeter of channel,
P_H: heated perimeter of channel, P_F: wetted perimeter of channel

indicated in Table 2 are the dependence of heat flux, mass velocity, and quality on the two-phase heat transfer coefficient, as well as the dominant heat transfer mechanism as suggested by the original authors. The 10,805 point database includes 9576 single-channel and 1229 multi-channel data points.

The database includes a range of relative roughness that is deemed to have minimal influence on dryout incipience quality. For the database of Ohta et al. [48], data exhibiting flow rate fluctuations at the test section inlet are excluded from the database. Only pure liquid data from the database of Li et al. [61] are included; any refrigerant mixture data are excluded.

Any duplicate data in the original databases are carefully identified and excluded from the consolidated database. Data points are also excluded that exhibit strong departure from the majority of comparable data. These include R507A data from Greco [44], and data of welded stainless steel tubes from Mahmoud et al. [57] and Karayiannis et al. [60]. It should be noted that the database is closely inspected by relying on published data from original sources.

The present pre-dryout heat transfer database includes a broad range of reduced pressures, from 0.005 to 0.69. The high pressure data include those of Yun et al. [36], P_R = 0.09–0.61, Yun et al. [39], P_R = 0.54, Mastrullo et al. [47], P_R = 0.38–0.55, Ducoulombier [50], P_R = 0.36–0.47, Oh and Son [31], P_R = 0.54–0.69, and Wu et al. [59], P_R = 0.14–0.47.

In all, the present pre-dryout database includes 10,805 saturated two-phase heat transfer coefficient data points with the following coverage:

- Working fluid: FC72, R11, R113, R123, R1234yf, R1234ze, R134a, R152a, R22, R236fa, R245fa, R32, R404A, R407C, R410A, R417A, CO_2, and water
- Hydraulic diameter: $0.19 < D_h < 6.5$ mm
- Mass velocity: $19 < G < 1608$ kg/m^2 s
- Liquid-only Reynolds number: $57 < Re_{fo} = GD_h/\mu_f < 49{,}820$
- Flow quality: $0 < x < 1$
- Reduced pressure: $0.005 < P_R < 0.69$.

3. Assessment of previous correlations

When comparing the consolidated database to predictions of previous models or correlations, the thermophysical properties for different fluids are obtained using NIST's REFPROP 8.0 software [75], excepting those for FC-72, which are obtained from 3M Company. Three different parameters are used to assess the accuracy of

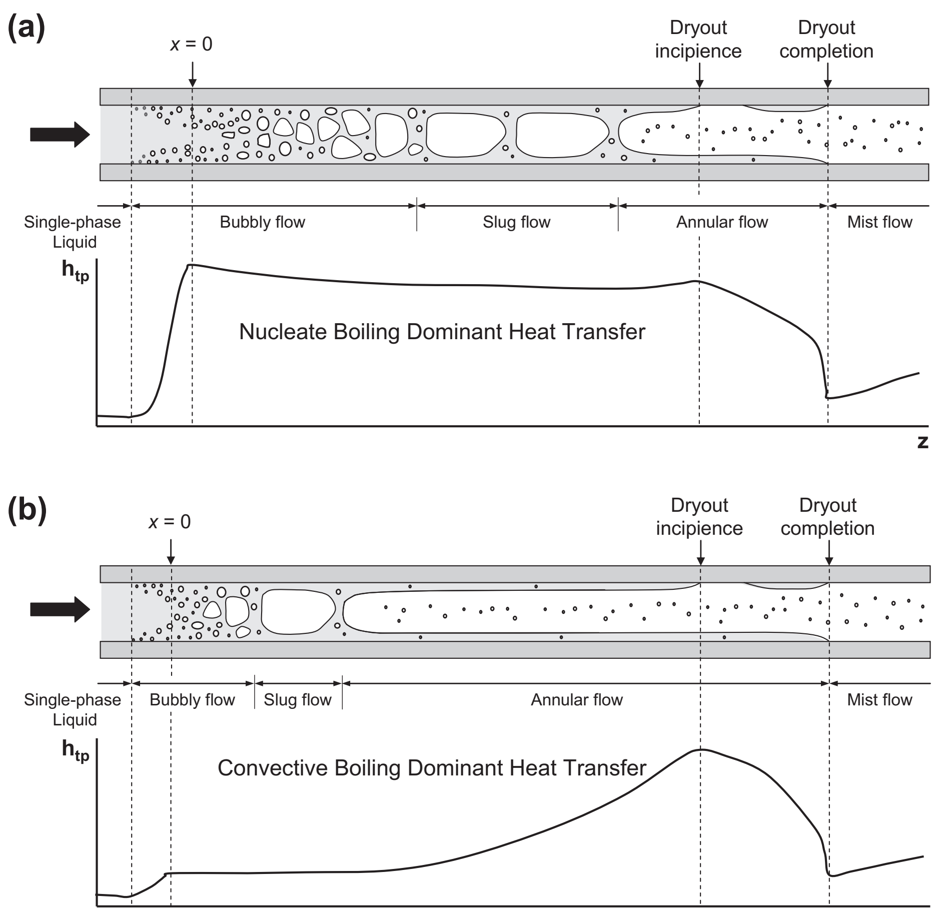

Fig. 1. Schematics of flow regimes, wall dryout and variation of heat transfer coefficient along uniformly heated channel for (a) nucleate boiling dominant heat transfer and (b) convective boiling dominant heat transfer [25].

Table 2
Saturated flow boiling heat transfer data for mini/micro-channels included in consolidated database.

Author(s)	Channel geometry[a]	Channel material	D_h [mm]	Relative roughness, e/D_h	Fluid(s)	G [kg/m^2 s]	Heat transfer characteristics[b]	Total data	Pre-dryout data[c]
Wambsganss et al. [32]	C single, H	Stainless steel	2.92	Smooth	R113	50–300	$h_{tp} = f(q'')$, NB	92	76
Tran [33]	C single, H	Brass	2.46	Smooth	R134a	33–502	$h_{tp} = f(q'')$, NB	302	302
Wang et al. [34]	C single, H	Copper	6.5	Smooth	R22	100–400	$h_{tp} = f(q'', G, x)$, NB + CB	63	61
Yan and Lin [35]	C multi, H	Copper	2.0	–	R134a	50–200	$h_{tp} = f(q'', G, x)$	137	116
Bao et al. [29]	C single, H	Copper	1.95	Smooth	R11, R123	167–560	$h_{tp} = f(q'')$, NB	164	143
Qu and Mudawar [26]	R multi, H	Copper + Lexan cover	0.349	–	Water	135–402	$h_{tp} = f(G, x)$, CB	335	335
Sumith et al. [27]	C single, VU	Stainless steel	1.45	–	Water	23–153	$h_{tp} = f(q'', G, x)$, CB	85	85
Yun et al. [36]	C single, H	Stainless steel	6.0	Smooth	R134a, CO_2	170–340	$h_{tp} = f(q'', G, x)$, NB	182	169
Huo et al. [30]	C single, VU	Stainless steel	2.01, 4.26	0.0009, 0.0004	R134a	100–500	$h_{tp} = f(q'', x)$, NB	365	323
Lee and Mudawar [37]	R multi, H	Copper + Lexan cover	0.349	–	R134a	61–657	$h_{tp} = f(q'', x)$, NB + CB	111	63
Saitoh et al. [38]	C single, H	Stainless steel	0.51, 1.12, 3.1	Smooth	R134a	150, 300	$h_{tp} = f(q'', G, x)$, NB + CB	420	259
Yun et al. [39]	R multi, H	Stainless steel	1.14, 1.53, 1.54	–	CO_2	200–400	$h_{tp} = f(q'', x)$, NB	57	43
Muwanga and Hassan [40]	C single, H	Stainless steel	1.067	–	FC72	770–1040	$h_{tp} = f(q'', G)$	454	327
Zhao and Bansal [41]	C single, H	Stainless steel	4.57	Smooth	CO_2	140–231	$h_{tp} = f(q'', G, x)$	22	19
Agostini et al. [42]	R multi, H	Silicon + Lexan cover	0.336	0.0005	R236fa	281–1370	$h_{tp} = f(q'', x)$, NB	593	458
Consolini [43]	C single, H	Stainless steel	0.51, 0.79	0.0047, 0.0022	R134a, R236fa, R245fa	274–1435	$h_{tp} = f(q'', x)$	650	585
Greco [44]	C single, H	Stainless steel	6.0	Smooth	R134a, R22, R404A, R407C, R410A, R417A	199–1100	$h_{tp} = f(q'', G, x)$, NB + CB	516	491
Bertsch et al. [45]	R multi, H	Copper + Lexan cover	0.544, 1.089	<0.0009, <0.0006	R134a, R245fa	19–336	$h_{tp} = f(q'' x)$, NB	332	214
In and Jeong [46]	C single, H	Stainless steel	0.19	–	R123, R134a	314–470	$h_{tp} = f(q'', G, x)$, NB + CB	256	159
Mastrullo et al. [47]	C single, H	Stainless steel	6.0	Smooth	CO_2	200–349	$h_{tp} = f(q'', x)$, NB	143	135
Ohta et al. [48]	C single, H	Stainless steel	0.51	–	FC72	107, 215	-	24	13
Wang et al. [49]	C single, H	Stainless steel	1.3	–	R134a	321–836	$h_{tp} = f(q'', x)$, NB	365	322
Ducoulombier [50]	C single, H	Stainless steel	0.529	0.0015–0.0030	CO_2	200–1400	$h_{tp} = f(q'', G, x)$, NB + CB	1573	1080
Hamdar et al. [51]	R single, H	Aluminum	1.0	–	R152a	210–580	$h_{tp} = f(q''$, NB	50	45
Martín-Callizo [52]	C single, VU	Stainless steel	0.64	0.0012	R134a, R22	185–535	$h_{tp} = f(q'', x)$	381	335
Ong [53]	C single, H	Stainless steel	1.03, 2.20, 3.04,	0.0006, 0.0004, 0.0003	R134a, R236fa, R245fa,	199–1608	$h_{tp} = f(q'', G, x)$, NB + CB	2504	2247
Tibiriçá and Ribatski [54]	C single, H	Stainless steel	2.32	0.0001	R134a, R245fa	50–700	$h_{tp} = f(q'', G, x)$, NB + CB	130	96
Ali et al. [55]	C single, VU	Stainless steel	1.7	0.0001	R134a	75–600	$h_{tp} = f(q'', x)$, NB	152	136
Bang et al. [28]	C single, H	Stainless steel	1.73	–	Water	100	$h_{tp} = f(x)$, CB	65	65
Copetti et al. [56]	C single, H	Stainless steel	2.62	0.0008	R134a	240–932	$h_{tp} = f(q'', G, x)$	876	845
Mahmoud et al. [57]	C single, VU	Stainless steel	1.1	0.0012	R134a	128–549	$h_{tp} = f(q'')$, NB	152	134
Oh and Son [31]	C single, H	Stainless steel	4.57	Smooth	CO_2	400–900	$h_{tp} = f(q'', x)$, NB	107	62
Oh and Son [58]	C single, H	Copper	1.77, 3.36, 5.35	Smooth	R134a, R22	200–500	$h_{tp} = f(G, x)$, CB	153	131
Wu et al. [59]	C single, H	Stainless steel	1.42	–	CO_2	300–600	$h_{tp} = f(q'', G, x)$, NB + CB	419	297
Karayiannis et al. [60]	C single, VU	Stainless steel	1.1	0.0012	R134a	215–550	$h_{tp} = f(q'', G, x)$, NB	545	489
Li et al. [61]	C single, H	Stainless steel	2.0	Smooth	R1234yf, R32	100–400	$h_{tp} = f(q'', G, x)$, NB + CB	169	134
Tibiriçá et al. [62]	C single, H	Stainless steel	1.0, 2.2	0.0006, 0.0004	R1234ze	300–600	$h_{tp} = f(G, x)$	30	11
Total								12,974	10,805

[a] C: circular, R: rectangular, H: horizontal, VU: vertical upward.
[b] NB: nucleate boiling dominant data as designated by original authors, CB: convective boiling dominant data as designated by original authors.
[c] Pre-dryout data corresponding to $x < x_{di}$ based on Table 1.

Table 3
Previous saturated flow boiling heat transfer correlations[a].

Author(s)	Equation	Remarks
Lazarek and Black [67]	$h_{tp} = (30Re_{fo}^{0.857}Bo^{0.714})(\frac{k_f}{D_h})$, $Re_{fo} = \frac{GD_h}{\mu_f}$, $Bo = \frac{q''_H}{Gh_{fg}}$	D = 3.15 mm, R113, nucleate boiling dominant
Shah [63]	$h_{tp} = max(E, S)h_{sp}$, $h_{sp} = 0.023Re_f^{0.8}Pr_f^{0.4}\frac{k_f}{D_h}$, for $N > 1.0$, $S = 1.8/N^{0.8}$, $E = 230Bo^{0.5}$ for $Bo > 3 \times 10^{-5}$, or $E = 1 + 46Bo^{0.5}$ for $Bo < 3 \times 10^{-5}$, for $0.1 < N \leqslant 1.0, S = 1.8/N^{0.8}, E = FBo^{0.5}\exp(2.74N^{-0.1})$, for $N \leqslant 0.1, S = 1.8/N^{0.8}, E = FBo^{0.5}\exp(2.47N^{-0.15})$, $F = 14.7$ for $Bo \geqslant 11 \times 10^{-4}$, or $F = 15.43$ for $Bo < 11 \times 10^{-4}$, $N = Co$ for vertical tube, $N = Co$ for horizontal tube with $Fr_f \geqslant 0.04$, $N = 0.38Fr_f^{-0.3}Co$ for horizontal tube with $Fr_f < 0.04$, $Re_f = \frac{G(1-x)D_h}{\mu_f}$, $Co = \left(\frac{1-x}{x}\right)^{0.8}\left(\frac{\rho_g}{\rho_f}\right)^{0.5}$, $Fr_f = \frac{G^2}{\rho_f^2 gD_h}$	D = 6–25.4 mm, water, R11, R12, R22, R113, cyclohexane, 780 data points
Cooper [64]	$h_{tp} = 55P_R^{0.12}(-log_{10}(P_R))^{-0.55}M^{-0.5}q_H''^{0.67}$	6000 data points for nucleate pool boiling
Gungor and Winterton [65]	$h_{tp} = Eh_{sp} + Sh_{nb}$, $h_{sp} = 0.023Re_f^{0.8}Pr_f^{0.4}\frac{k_f}{D_h}$, $E = 1 + 24000Bo^{1.16} + 1.37\left(\frac{1}{X_{tt}}\right)^{0.86}$, $h_{nb} = h_{tp,Cooper}$, $S = \left(1 + 1.15 \times 10^{-6}E^2Re_f^{1.17}\right)^{-1}$, for horizontal tube with $Fr_f \leqslant 0.05$, replace E and S with $EFr_f^{(0.1-2Fr_f)}$ and $SFr_f^{0.5}$, respectively	D = 2.95–32.0 mm, water, R11, R12, R113, R114, R22, ethylene glycol, 4300 data points
Liu and Winterton [66]	$h_{tp} = [(Eh_{sp})^2 + (Sh_{nb})^2]^{0.5}$, $h_{sp} = 0.023Re_{fo}^{0.8}Pr_f^{0.4}\frac{k_f}{D_h}$, $E = \left[1 + xPr_f(\frac{\rho_f}{\rho_g} - 1)\right]^{0.35}$, $h_{nb} = h_{tp,Cooper}$, $S = \left(1 + 0.055E^{0.1}Re_{fo}^{0.16}\right)^{-1}$, for horizontal tube with $Fr_f \leqslant 0.05$, replace E and S with $EFr_f^{(0.1-2Fr_f)}$ and $SFr_f^{0.5}$, respectively	Same data as Gungor and Winterton's [65]
Tran et al. [68]	$h_{tp} = 8.4 \times 10^5\left(Bo^2We_{fo}\right)^{0.3}\left(\frac{\rho_g}{\rho_f}\right)^{0.4}$, $We_{fo} = \frac{G^2D_h}{\rho_f\sigma}$	D = 2.46, 2.92 mm, D_h = 2.40 mm, R12, R113, nucleate boiling dominant
Warrier et al. [69]	$h_{tp} = Eh_{sp}$, $h_{sp} = 0.023Re_{fo}^{0.8}Pr_f^{0.4}\frac{k_f}{D_h}$, $E = 1.0 + 6.0Bo^{1/16} - 5.3(1 - 855Bo)x^{0.65}$	D_h = 0.75 mm, five parallel, FC84
Yu et al. [70]	$h_{tp} = 6.4 \times 10^6(Bo^2We_{fo})^{0.27}\left(\frac{\rho_g}{\rho_f}\right)^{0.2}$	D = 2.98 mm, water, ethylene glycol, nucleate boiling dominant
Agostini and Bontemps [71]	$h_{tp} = 28q_H''^{2/3}G^{-0.26}x^{-0.10}$ for $x < 0.43$, $h_{tp} = 28q_H''^{2/3}G^{-0.64}x^{-2.08}$ for $x > 0.43$	D_h = 2.01 mm, 11 parallel, R134a
Bertsch et al. [72]	$h_{tp} = Eh_{cb} + Sh_{nb}$, $h_{cb} = h_{sp,fo}(1 - x) + h_{sp,go}x$, $E = 1 + 80(x^2 - x^6)\exp(-0.6N_{conf})$, $h_{nb} = h_{tp,Cooper}$, $S = 1 - x$, $N_{conf} = \sqrt{\frac{\sigma}{g(\rho_f-\rho_g)D_h^2}}$, $h_{sp,fo} = \left(3.66 + \frac{0.0668\frac{D_h}{L}Re_{fo}Pr_f}{1+0.04\left[\frac{D_h}{L}Re_{fo}Pr_f\right]^{2/3}}\right)\frac{k_f}{D_h}$, $h_{sp,go} = \left(3.66 + \frac{0.0668\frac{D_h}{L}Re_{go}Pr_g}{1+0.04[\frac{D_h}{L}Re_{go}Pr_g]^{2/3}}\right)\frac{k_g}{D_h}$, $Re_{fo} = \frac{GD_h}{\mu_f}$, $Re_{go} = \frac{GD_h}{\mu_g}$	D_h = 0.16–2.92 mm, water, refrigerants, FC-77, nitrogen, 3899 data points
Li and Wu [73]	$h_{tp} = 334Bo^{0.3}\left(BdRe_f^{0.36}\right)^{0.4}\frac{k_f}{D_h}$, $Bd = \frac{g(\rho_f-\rho_g)D_h^2}{\sigma}$	D_h = 0.16–3.1 mm, water, refrigerants, FC-77, ethanol, propane, CO_2, 3744 data points
Ducoulombier et al. [74]	$h_{tp} = max(h_{nb}, h_{cb})$, $h_{nb} = 131P_R^{-0.0063}(-log_{10}(P_R))^{-0.55}M^{-0.5}q_H''^{0.58}$, if $Bo > 1.1 \times 10^{-4}$, $h_{cb} = \left[1.47 \times 10^4Bo + 0.93\left(\frac{1}{X_{tt}}\right)^{2/3}\right]\left(0.023Re_{fo}^{0.8}Pr_f^{1/3}\frac{k_f}{D_h}\right)$, if $Bo < 1.1 \times 10^{-4}$, $h_{cb} = \left[1 + 1.80\left(\frac{1}{X_{tt}}\right)^{0.986}\right]\left(0.023Re_f^{0.8}Pr_f^{0.4}\frac{k_f}{D_h}\right)$	D = 0.529 mm, CO_2
Oh and Son [58]	$h_{tp} = 0.034Re_f^{0.8}Pr_f^{0.3}[1.58(\frac{1}{X_{tt}})^{0.87}](\frac{k_f}{D_h})$	D = 1.77, 3.36, 5.35 mm, R134a, R22

[a] The Cooper [64] correlation was developed for nucleate pool boiling.

individual models or correlations. θ and ξ are defined as the percentages of data points predicted within ±30% and ±50%, respectively, and MAE the mean absolute error, which is determined according to

$$MAE = \frac{1}{N}\sum\frac{\left|h_{tp,pred} - h_{tp,\exp}\right|}{h_{tp,\exp}} \times 100\%. \tag{1}$$

Table 3 provides a summary of previous saturated flow boiling heat transfer correlations that have been recommended previously for macro-channels [63–66] and mini/micro-channels [58,67–74]. It should be emphasized that the correlations in Table 3 were derived for specific fluids and specific ranges of operating conditions. The Cooper [64] correlation, which was originally developed for nucleate pool boiling, has been recommended for nucleate flow boiling in several published works, such as those of Gungor and Winterton [65], Liu and Winterton [66], Bao et al. [29], Yun et al. [39], and Bertsch et al. [45,72]. The correlations of Lazarek and Black [67], Tran et al. [68], and Yu et al. [70] are based on their respective nucleate boiling dominant heat transfer data. The correlations of

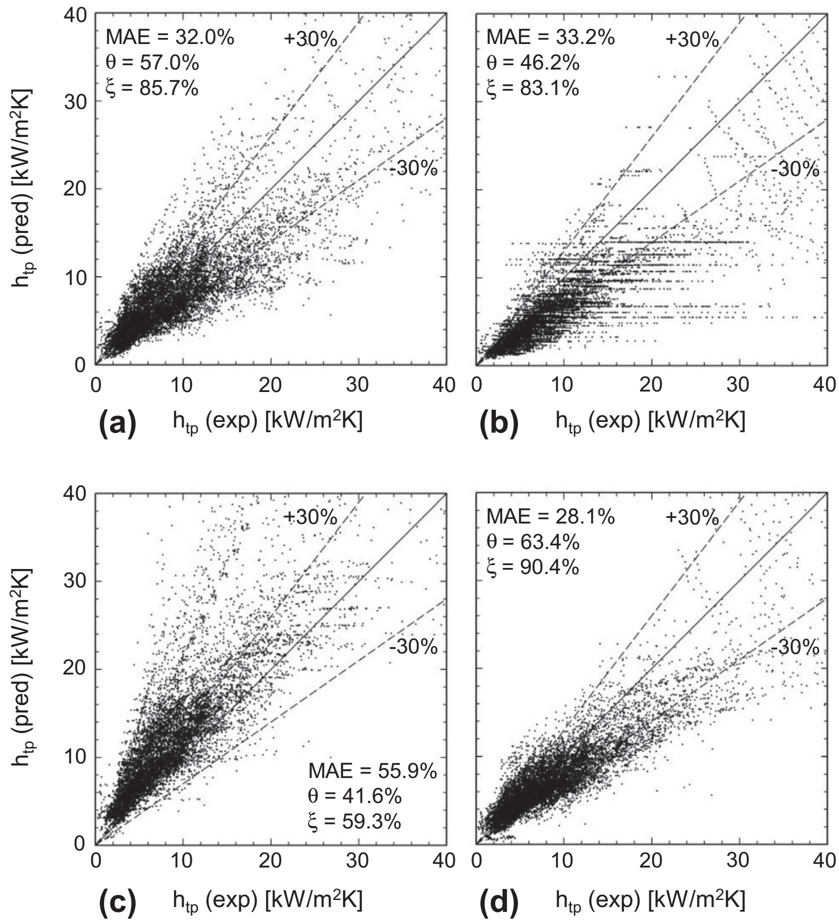

Fig. 2. Comparison of 10,805 pre-dryout data points with predictions of previous correlations recommended for macro-channels: (a) Shah [63], (b) Cooper [64], (c) Gungor and Winterton [65], and (d) Liu and Winterton [66].

Warrier et al. [69] and Agostini and Bontemps [71] were developed specially for multi-port mini/micro-channel test sections. Shah [63], Gungor and Winterton [65], and Liu and Winterton [66] proposed generalized correlations based on broad-range of databases for macro-channels, and Bertsch et al. [72], and Li and Wu [73] for mini/micro-channels.

Since the correlations in Table 3 are intended for uniform circumferential heating in circular tubes, or rectangular channels with four-sided heating, a multiplier is adopted when applying these correlations to saturated flow boiling data in rectangular channels with three-sided wall heating, such as those of Qu and Mudawar [26], Lee and Mudawar [37], Agostini et al. [42], and Bertsch et al. [45]. Following a technique adopted in Refs. [24,26,37,76], the saturated flow boiling heat transfer coefficient for three-sided heating is related to that for uniform circumferential heating by the relation

$$h_{tp} = \left(\frac{Nu_3}{Nu_4}\right) h_{tp,cir}, \tag{2}$$

where $h_{tp,cir}$ is the local heat transfer coefficient based on uniform circumferential heating obtained from Table 3, and Nu_3 and Nu_4 are Nusselt numbers for thermally developed laminar flow with three-sided and four-sided heat transfer [77], respectively,

$$Nu_3 = 8.235(1 - 1.833\beta + 3.767\beta^2 - 5.814\beta^3 + 5.361\beta^4 - 2.0\beta^5) \tag{3a}$$

and

$$Nu_4 = 8.235(1 - 2.042\beta + 3.085\beta^2 - 2.477\beta^3 + 1.058\beta^4 - 0.186\beta^5). \tag{3b}$$

Figs. 2 and 3 compare the 10,805 pre-dryout data points with predictions of previous empirical heat transfer correlations recommended for macro-channels [63–66] and mini/micro-channels [58,67–74], respectively.

Fig. 2 shows the previous heat transfer correlations recommended for macro-channels provide fair to poor predictions of the consolidate database. The correlation of Copper [64] generally underpredicts the database, while that of Gungor and Winterton [65] overpredicts the database. Most of the high pressure data are underpredicted by the Shah [63] and Liu and Winterton [66] correlations.

Fig. 3 shows most of the mini/micro-channel correlations produce large scatter against the consolidate database, especially those of Yu et al. [70] and Agostini and Bontemps [71]. The consolidated database is generally underpredicted by Lazarek and Black [67], and Bertsch et al. [72], significant underpredicted by Tran et al. [68], Warrier et al. [69], and Oh and Son [58], and significant overpredicted by Ducoulombier et al. [74]. The correlations of Lazarek and Black, Warrier et al., and Agostini and Bontemps overpredict most high pressure data.

Among all previous correlations for macro-channels and mini/micro-channels, those of Lazarek and Black, and Liu and Winterton show relatively fair predictions, but their accuracy is compromised against convective boiling dominant data and diameters below 0.5 mm.

4. New predictive method

The primary objective of this study is to develop a simple method to predicting the heat transfer coefficient for saturated

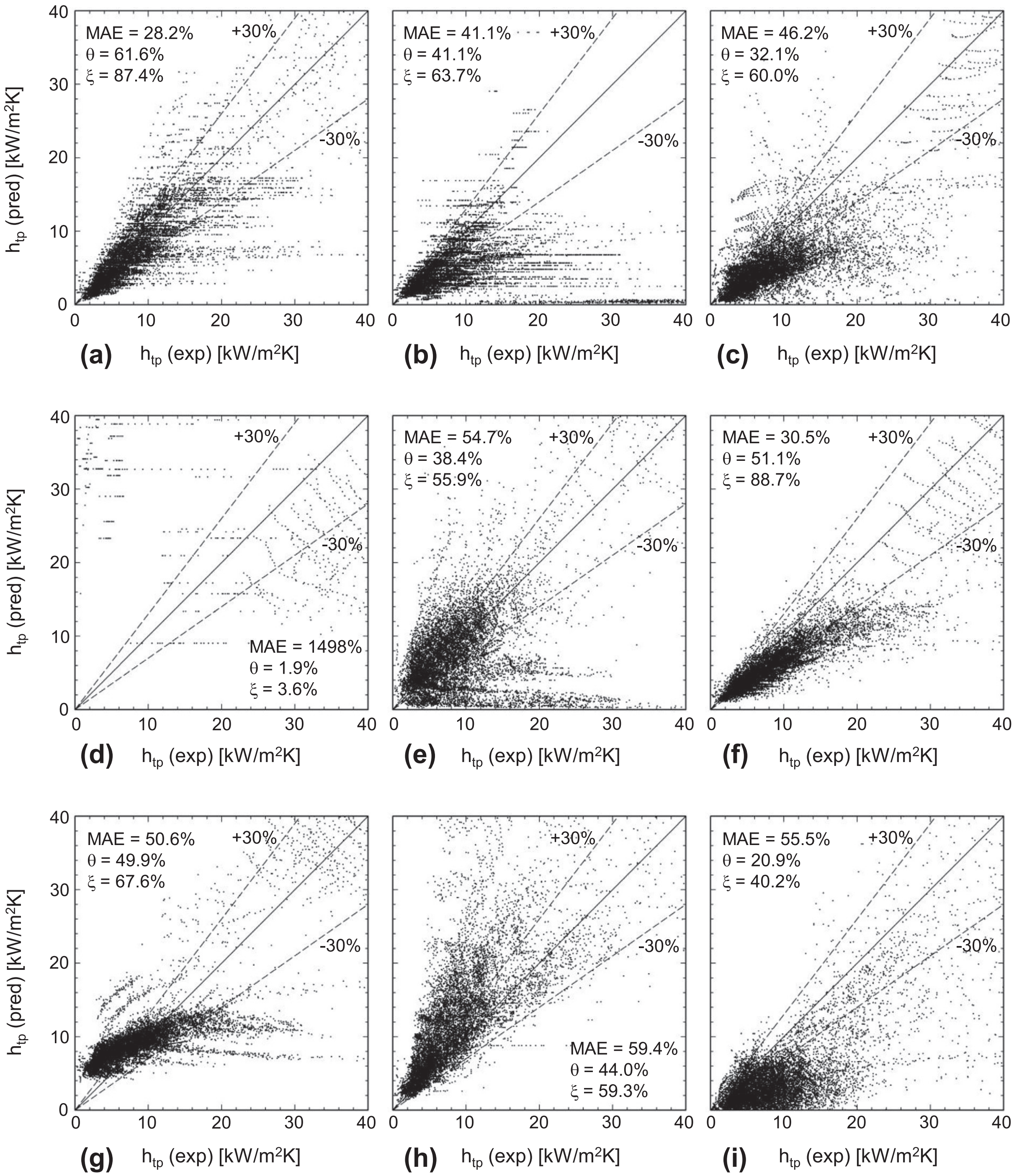

Fig. 3. Comparison of 10,805 pre-dryout data points with predictions of previous correlations recommended for mini/micro-channels: (a) Lazarek and Black [67], (b) Tran et al. [68], (c) Warrier et al. [69], (d) Yu et al. [70], (e) Agostini and Bontemps [71], (f) Bertsch et al. [72], (g) Li and Wu [73], (h) Ducoulombier et al. [74], and (i) Oh and Son [58].

Table 4
New correlation for pre-dryout saturated flow boiling heat transfer in mini/micro-channels.

$$h_{tp} = (h_{nb}^2 + h_{cb}^2)^{0.5}$$

$$h_{nb} = \left[2345\left(Bo\frac{P_H}{P_F}\right)^{0.70} P_R^{0.38}(1-x)^{-0.51}\right]\left(0.023Re_f^{0.8}Pr_f^{0.4}\frac{k_f}{D_h}\right)$$

$$h_{cb} = \left[5.2\left(Bo\frac{P_H}{P_F}\right)^{0.08} We_{fo}^{-0.54} + 3.5\left(\frac{1}{X_{tt}}\right)^{0.94}\left(\frac{\rho_g}{\rho_f}\right)^{0.25}\right]\left(0.023Re_f^{0.8}Pr_f^{0.4}\frac{k_f}{D_h}\right)$$

where $Bo = \frac{q''_H}{G h_{fg}}$, $P_R = \frac{P}{P_{crit}}$, $Re_f = \frac{G(1-x)D_h}{\mu_f}$, $We_{fo} = \frac{G^2 D_h}{\rho_f \sigma}$, $X_{tt} = \left(\frac{\mu_f}{\mu_g}\right)^{0.1}\left(\frac{1-x}{x}\right)^{0.9}\left(\frac{\rho_g}{\rho_f}\right)^{0.5}$,

q''_H: effective heat flux averaged over heated perimeter of channel, P_H: heated perimeter of channel, P_F: wetted perimeter of channel

boiling in mini/micro-channel flows with high accuracy. As discussed earlier, the correlations of Gungor and Winterton [65], Ducoulombier et al. [74], and Oh and Son [58], which where based on the popular functional form of Schrock and Grossman [78], yielded inferior predictions of the present consolidated database. Schrock and Grossman proposed the following form based on their experimental data for upward water flow in channels having diameters from 2.95 mm to 10.97 mm,

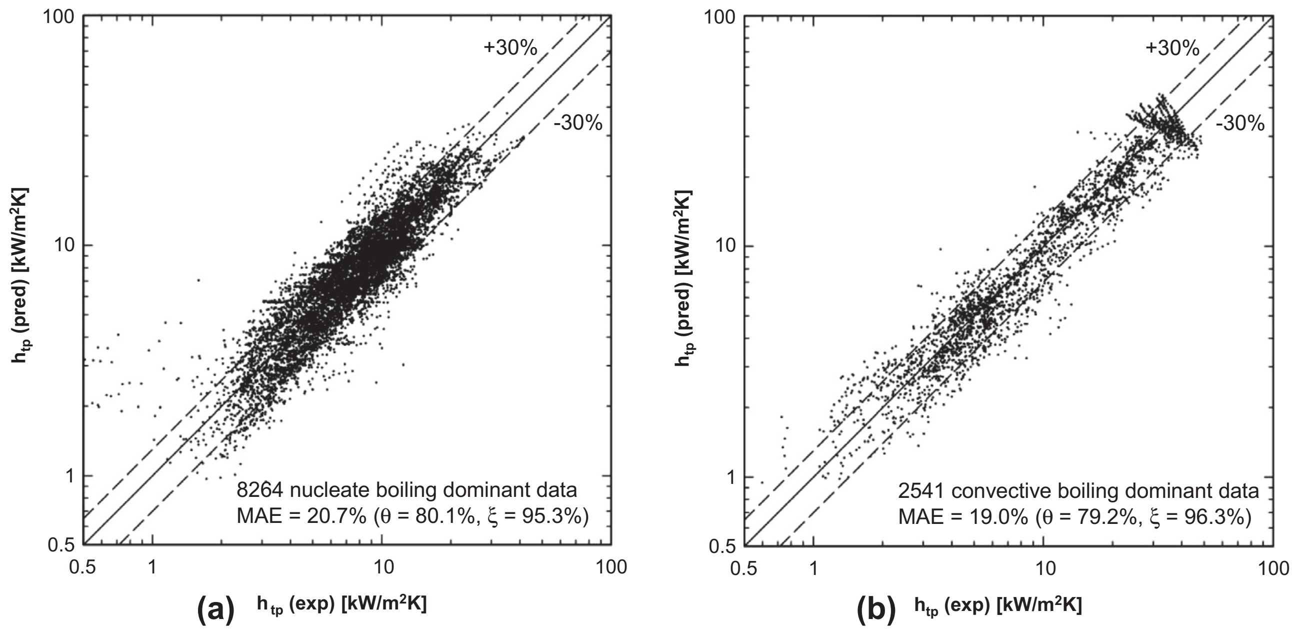

Fig. 4. Comparison of predictions of new correlation with two subsets of 10,805 point pre-dryout database corresponding to: (a) nucleate boiling dominant data and (b) convective boiling dominant data. Nucleate boiling dominant data correspond to $h_{nb}/h_{cb} > 1.0$, where h_{nb} and h_{cb} are calculated using Table 4.

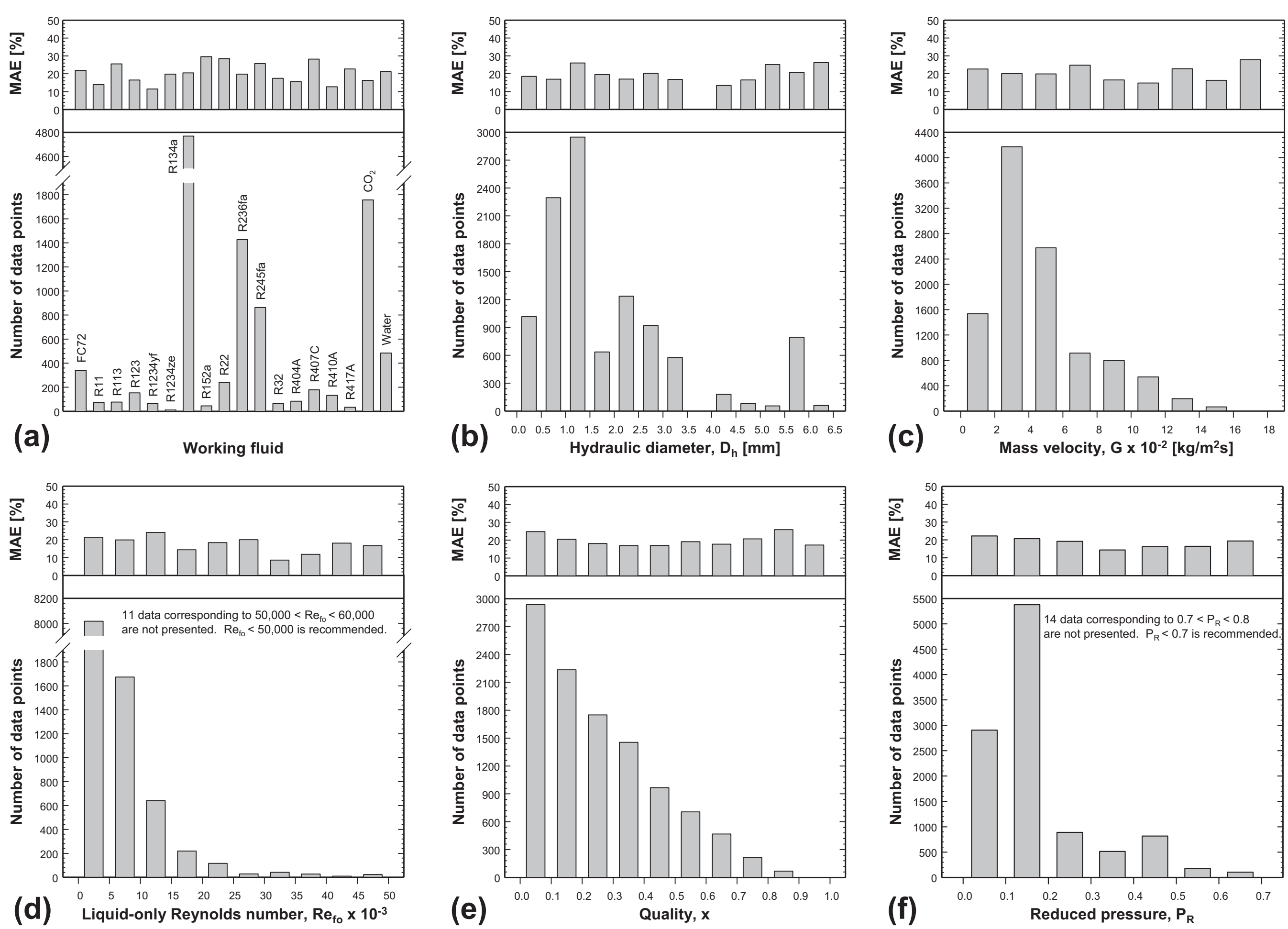

Fig. 5. Distributions of number of data points and MAE in predictions of new correlation method for 10,805 point pre-dryout database relative to: (a) working fluid, (b) hydraulic diameter, (c) mass velocity, (d) liquid-only Reynolds number, (e) quality, and (f) reduced pressure.

Table 5
Comparison of individual mini/micro-channel pre-dryout heat transfer databases with predictions of present and select previous correlations.

Author(s)	D_h [mm]	Fluid(s)	$(h_{nb}/h_{cb})_{avg}$ [a]	Mean absolute error [%]				
				Lazarek and Black [67]	Shah [63]	Liu and Winterton [66]	Bertsch et al. [72]	New correlation
Wambsganss et al. [32]	2.92	R113	2.12	20.0	21.6	27.2	19.6	25.5
Tran [33]	2.46	R134a	1.71	31.5	30.8	27.5	31.0	23.1
Wang et al. [34]	6.5	R22	0.65	26.5	33.2	33.6	27.9	26.2
Yan and Lin [35]	2.0	R134a	1.44	35.9	31.0	23.7	24.2	21.8
Bao et al. [29]	1.95	R11, R123	5.24	9.6	18.6	28.8	29.6	14.2
Qu and Mudawar [26]	0.349	Water	0.26	41.0	61.8	41.8	19.5	20.5
Sumith et al. [27]	1.45	Water	0.21	36.4	35.3	31.1	40.2	28.6
Yun et al. [36]	6.0	R134a, CO_2	2.37	33.1	39.8	23.9	24.4	24.0
Huo et al. [30]	2.01, 4.26	R134a	7.92	16.0	34.3	28.1	25.6	13.6
Lee and Mudawar [37]	0.349	R134a	2.93	12.6	21.7	41.5	46.9	26.2
Saitoh et al. [38]	0.51, 1.12, 3.1	R134a	0.72	30.7	17.3	19.6	31.1	14.4
Yun et al. [39]	1.14, 1.53, 1.54	CO_2	2.00	26.7	45.4	20.9	24.0	18.6
Muwanga and Hassan [40]	1.067	FC72	6.80	19.2	40.4	30.9	42.7	22.4
Zhao and Bansal [41]	4.57	CO_2	1.16	12.4	15.7	14.6	26.6	10.2
Agostini et al. [42]	0.336	R236fa	3.35	34.4	52.1	36.9	25.1	17.8
Consolini [43]	0.51, 0.79	R134a, R236fa, R245fa	3.55	14.9	30.7	32.5	33.1	14.9
Greco [44]	6.0	R134a, R22, R404A, R407C, R410A, R417A	1.00	28.5	41.1	50.2	36.5	21.0
Bertsch et al. [45]	0.544, 1.089	R134a, R245fa	3.34	46.3	24.0	26.4	22.4	22.0
In and Jeong [46]	0.19	R123, R134a	0.77	40.9	32.3	42.6	45.8	13.0
Mastrullo et al. [47]	6.0	CO_2	2.08	19.9	34.9	14.0	13.3	15.5
Ohta et al. [48]	0.51	FC72	1.14	27.0	29.2	17.6	21.3	11.0
Wang et al. [49]	1.3	R134a	2.65	24.6	23.3	26.8	44.3	17.2
Ducoulombier [50]	0.529	CO_2	1.34	37.5	29.1	23.9	38.3	15.9
Hamdar et al. [51]	1.0	R152a	1.11	39.5	29.0	22.7	46.7	29.6
Martín-Callizo [52]	0.64	R134a, R22	2.91	15.3	9.3	15.8	23.1	19.8
Ong [53]	1.03, 2.20, 3.04,	R134a, R236fa, R245fa,	3.64	25.3	33.9	23.8	21.9	24.7
Tibiriçá and Ribatski [54]	2.32	R134a, R245fa	0.91	37.2	13.6	15.5	31.3	17.8
Ali et al. [55]	1.7	R134a	4.79	29.6	39.5	34.2	31.8	28.7
Bang et al. [28]	1.73	Water	0.36	29.8	31.4	20.1	25.2	15.1
Copetti et al. [56]	2.62	R134a	3.18	25.0	19.2	21.0	29.2	19.8
Mahmoud et al. [57]	1.1	R134a	4.94	23.2	36.5	41.9	40.3	16.7
Oh and Son [31]	4.57	CO_2	10.00	12.4	36.5	7.1	22.0	18.4
Oh and Son [58]	1.77, 3.36, 5.35	R134a, R22	1.52	33.3	26.6	25.1	37.4	21.8
Wu et al. [59]	1.42	CO_2	1.42	41.3	34.6	25.0	30.8	16.4
Karayiannis et al. [60]	1.1	R134a	3.20	31.1	36.9	43.0	47.0	28.2
Li et al. [61]	2.0	R1234yf, R32	0.73	40.2	21.9	19.5	42.6	14.5
Tibiriçá et al. [62]	1.0, 2.2	R1234ze	1.82	10.0	14.7	11.7	19.5	19.8
Total				28.2	32.0	28.1	30.5	20.3

[a] Average value of h_{nb}/h_{cb} for individual database, where h_{nb} and h_{cb} are calculated using Table 4.

$$h_{tp} = \left[C_1 Bo + C_2\left(\frac{1}{X_{tt}}\right)^{2/3}\right]\left(0.023 Re_{fo}^{0.8} Pr_f^{0.4}\frac{k_f}{D_h}\right), \tag{4}$$

where Bo and X_{tt} are the Boiling number and Lockhart–Martinelli parameter [79] based on turbulent liquid-turbulent vapor flows, respectively. The first and second terms in the first multiplier in Eq. (4) reflect the influences of the nucleate boiling dominant and convective boiling dominant regimes, respectively. The second multiplier is the Dittus-Boetler single-phase heat transfer coefficient relation based on Re_{fo}.

An alternative strategy adopted in the present study is to utilize the general functional form of Schrock and Grossman, but with the Dittus-Boetler relation based on Re_f. The following relation is proposed to predict the heat transfer coefficient for the nucleate boiling dominant regime,

$$h_{nb} = \left[C_3\left(Bo\frac{P_H}{P_F}\right)^{N_1} P_R^{N_2}(1-x)^{-N_3}\right]\left(0.023 Re_f^{0.8} Pr_f^{0.4}\frac{k_f}{D_h}\right), \tag{5a}$$

and for the convective boiling dominant regime,

$$h_{cb} = \left[C_4\left(Bo\frac{P_H}{P_F}\right)^{N_4} We_{fo}^{N_5} + C_5\left(\frac{1}{X_{tt}}\right)^{N_6}\left(\frac{\rho_g}{\rho_f}\right)^{N_7}\right]\left(0.023 Re_f^{0.8} Pr_f^{0.4}\frac{k_f}{D_h}\right), \tag{5b}$$

Notice that the term including X_{tt} in Eq. (4) is deliberately omitted from Eq. (5a) due to its negligible influence in the nucleate boiling dominant regime. To account for nucleate boiling suppression, the term $(1-x)^{-N_3}$ is introduced in Eq. (5a). The reduced pressure and density ratio terms are used to both cope with the drastically different thermophysical properties of the different working fluids (FC72, refrigerants, CO_2, and water) and broad range of operating

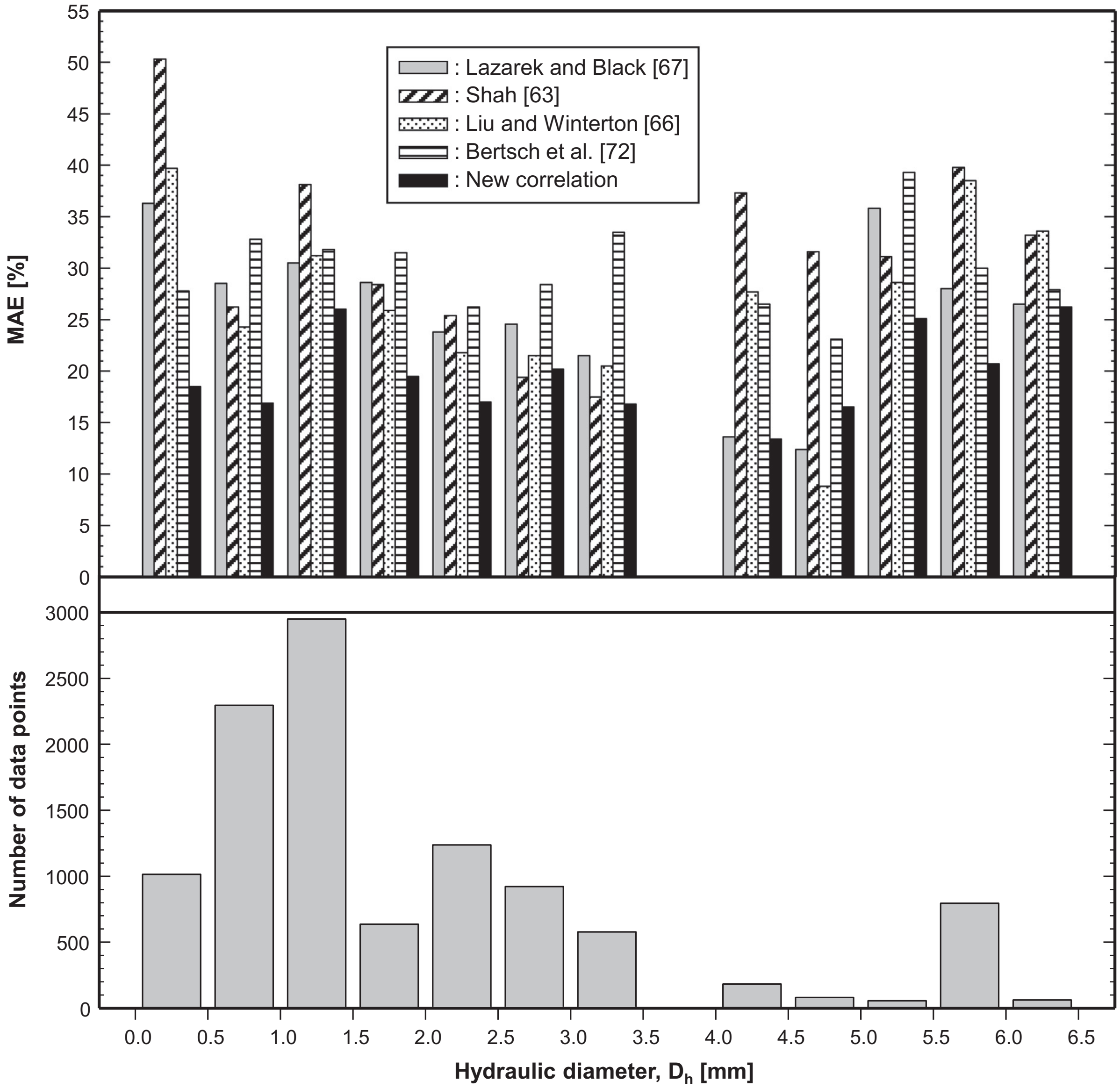

Fig. 6. Distribution of MAE in predictions of new correlation and select previous correlations for 10,805 point pre-dryout database relative to hydraulic diameter.

Table 6
Assessment of present correlation and select previous correlations against four subsets of 10,805 point pre-dryout database corresponding to refrigerants, water, CO_2, and FC72.

Author(s)	Refrigerants dryout incipience database (8222 points)			Water dryout incipience database (485 points)			CO_2 dryout incipience database (1758 points)			FC72 dryout incipience database (340 points)		
	MAE (%)	θ (%)	ξ (%)	MAE (%)	θ (%)	ξ (%)	MAE (%)	θ (%)	ξ (%)	MAE (%)	θ (%)	ξ (%)
Lazarek and Black [67]	26.5	66.4	89.8	38.7	45.2	69.7	34.8	40.7	79.9	19.5	77.9	93.8
Shah [63]	30.4	60.7	87.4	53.0	37.9	59.0	32.2	45.2	87.5	40.0	54.7	72.4
Liu and Winterton [66]	28.5	63.2	90.1	37.0	48.9	73.8	22.9	70.0	97.4	30.4	55.6	86.5
Bertsch et al. [72]	30.0	52.8	91.4	23.9	67.0	90.3	32.6	44.3	81.1	41.9	22.4	60.9
New correlation	21.0	79.2	95.2	21.2	72.2	98.4	16.3	87.0	97.7	21.9	70.9	87.6

pressure. The ratio of the flow channel's heated to wetted perimeters, P_H/P_F, is also considered to tackle three-sided wall heating (*e.g.*, Qu and Mudawar [26], Lee and Mudawar [37], Agostini et al. [42], and Bertsch et al. [45] in Table 2), instead of using the multiplier for three-sided heating, Eq. (2). Incorporating We_{fo} in Eq. 5(b) is intended to account for the influence of interactions between inertia and surface tension force since surface tension plays a more significant role in mini/micro-channels than in macro-channels; the Weber number is defined as

$$We_{fo} = \frac{G^2 D_h}{\rho_f \sigma}. \tag{6}$$

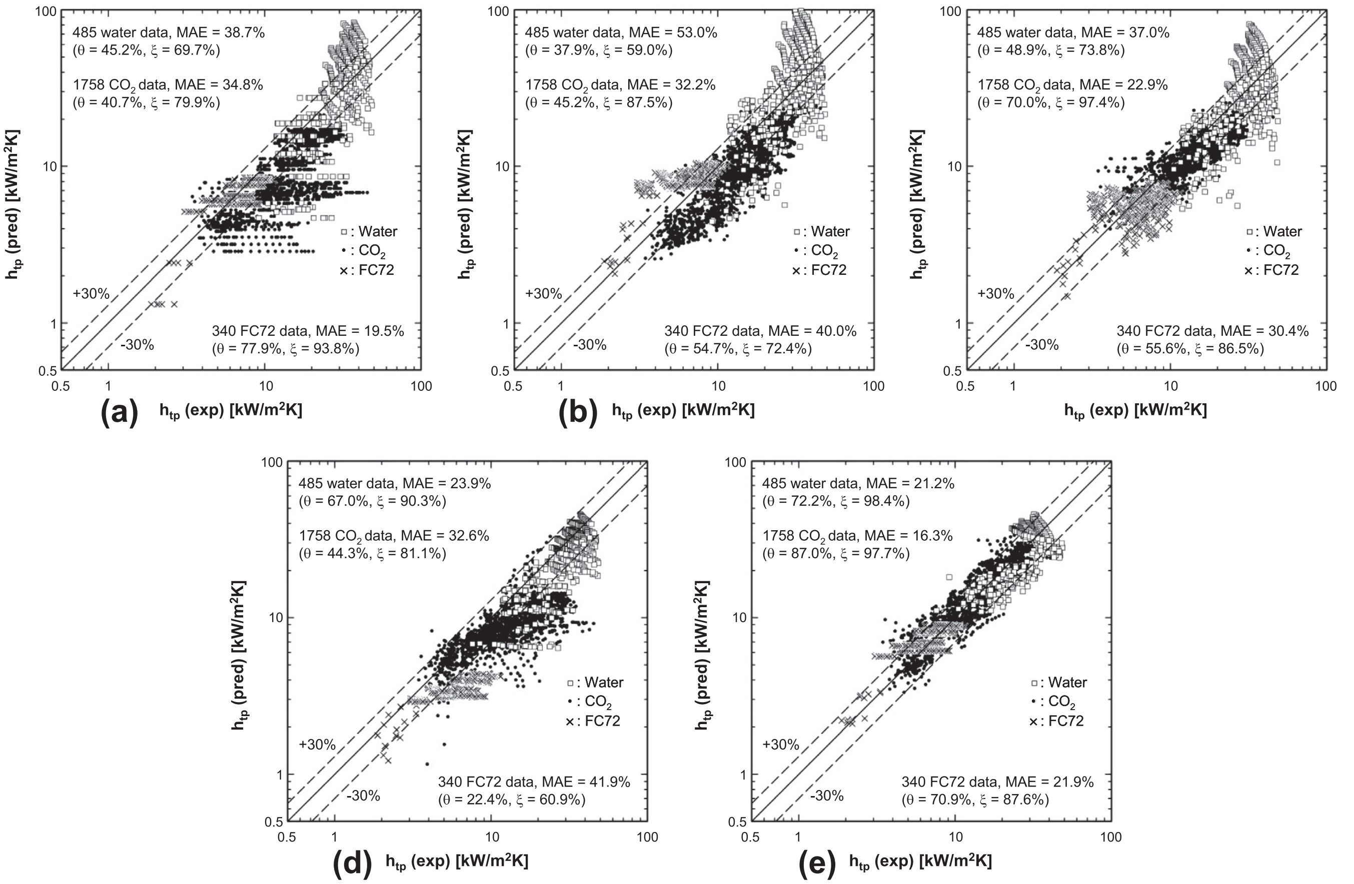

Fig. 7. Comparison of water, CO_2, and FC72 data of 10,805 point pre-dryout database with predictions of: (a) Lazarek and Black [67], (b) Shah [63], (c) Liu and Winterton [66], (d) Bertsch et al. [72], and (e) new correlation.

Table 7
Assessment of present correlation and previous correlations with two subsets of 10,805 point pre-dryout database corresponding to nucleate boiling dominant and convective boiling dominant heat transfer.

Author(s)	Nucleate boiling dominant database (8264 points)[a]			Convective boiling dominant database (2541 points)		
	MAE (%)	θ (%)	ξ (%)	MAE (%)	θ (%)	ξ (%)
Lazarek and Black [67]	24.3	71.3	93.0	40.6	30.1	69.0
Shah [63]	31.3	57.0	86.9	34.2	56.8	81.9
Cooper [64]	29.7	53.6	90.6	44.6	22.1	58.8
Gungor and Winterton [65]	58.9	39.7	56.8	46.0	47.9	67.5
Liu and Winterton [66]	26.8	64.8	92.7	32.0	59.1	82.9
Tran et al. [68]	34.1	49.1	73.8	64.0	15.5	30.6
Warrier et al. [69]	43.1	36.1	67.0	56.2	19.2	37.4
Yu et al. [70]	1673	0.0	0.0	928.5	8.2	15.2
Agostini and Bontemps [71]	52.4	43.3	62.0	62.1	22.4	36.0
Bertsch et al. [72]	28.5	55.6	93.5	37.0	36.2	73.3
Li and Wu [73]	49.9	52.1	69.0	52.8	42.8	63.0
Ducoulombier et al. [74]	66.5	38.9	54.0	36.3	60.7	76.3
Oh and Son [58]	62.9	8.4	27.4	31.5	61.5	81.8
New correlation	20.7	80.1	95.3	19.0	79.2	96.3

[a] Nucleate boiling dominant data corresponding to $h_{nb}/h_{cb} > 1.0$, where h_{nb} and h_{cb} are calculated using Table 4.

A superposition of the Churchill and Usagi [80] type of h_{nb} and h_{cb} is used to obtain a single relation for the heat transfer coefficient,

$$h_{tp} = \left(h_{nb}^{N_8} + h_{cb}^{N_8}\right)^{1/N_8}. \tag{7}$$

Based on the entire 10,805 point pre-dryout database for saturated flow boiling in mini/micro-channels, the following simple relations, which are also detailed in Table 4, are proposed for predicting saturated flow boiling heat transfer coefficient, where all the empirical constants are determined by minimizing MAE against the database,

$$h_{tp} = \left(h_{nb}^2 + h_{cb}^2\right)^{0.5}, \tag{8a}$$

where

$$h_{nb} = \left[2345\left(Bo\frac{P_H}{P_F}\right)^{0.70} P_R^{0.38}(1-x)^{-0.51}\right]\left(0.023Re_f^{0.8}Pr_f^{0.4}\frac{k_f}{D_h}\right), \tag{8b}$$

and

$$h_{cb} = \left[5.2\left(Bo\frac{P_H}{P_F}\right)^{0.08} We_{fo}^{-0.54} + 3.5\left(\frac{1}{X_{tt}}\right)^{0.94}\left(\frac{\rho_g}{\rho_f}\right)^{0.25}\right]\left(0.023Re_f^{0.8}Pr_f^{0.4}\frac{k_f}{D_h}\right), \tag{8c}$$

where the Boiling number is expressed in terms of q''_H, the effective heat flux averaged over the heated perimeter of the channel,

$$Bo = \frac{q''_H}{Gh_{fg}}. \tag{9}$$

Fig. 4(a) and (b) shows predictions of the new saturated boiling heat transfer correlations compared to two subsets of the 10,805 point pre-dryout database: nucleate boiling dominant data and convective boiling dominant data, respectively. Notice that the nucleate boiling dominant data correspond to $h_{nb}/h_{cb} > 1.0$, where h_{nb} and h_{cb} are calculated using Table 4. The MAE for the 8264 data nucleate boiling dominant subset is 20.7%, with 80.1% and 95.3% of the data falling within ±30% and ±50% error bands, respectively. The corresponding values for the 2541 data convective boiling dominant subset are MAE of 19.0%, and 79.2% and 96.3% of the data falling within ±30% and ±50% error bands, respectively. The overall MAE for the entire 10,805 point pre-dryout database is 20.3%, with 79.9% and 95.5% of the data falling within ±30% and ±50% error bands, respectively.

Achieving low MAE values is an incomplete measure of the effectiveness of a correlation. A more definitive measure is good predictive accuracy over broad ranges of individual flow parameters. As discussed in [20–24], this notion is overlooked in most studies involving the development of two-phase pressure drop and heat transfer correlations.

Fig. 5 shows, for each parameter, both a lower bar chart distribution of number of data points, and corresponding upper bar chart distribution of MAE in the prediction of the new saturated boiling heat transfer correlation. The distribution of the entire 10,805 point pre-dryout database is examined relative to working fluid, hydraulic diameter, D_h, mass velocity, G, liquid-only Reynolds number, Re_{fo}, quality, x, and reduced pressure, P_R. Overall, the new correlation shows very good predictions for most parameter bins, evidenced by MAE values generally around 20%. Notice that the parameter ranges corresponding to $50{,}000 < Re_{fo} < 60{,}000$ and $0.7 < P_R < 0.8$ are not recommended, since data numbers in those ranges are very sparse to ascertain the accuracy of the present correlation.

Another measure of the predictive accuracy of the new correlation is the ability to provide evenly good predictions for individual databases comprising the consolidated database. Table 5 compares individual mini/micro-channel databases from 37 sources with predictions of the present correlation as well as select previous correlations that have shown relatively superior predictive capability. Average values of h_{nb}/h_{cb} of individual databases are also presented in Table 5, where h_{nb} and h_{cb} are calculated using the present correlation as indicated in Table 4; a large value of $(h_{nb}/h_{cb})_{avg}$ indicates nucleate boiling is the dominant heat transfer regime, while a small value indicates convective boiling associated with annular film evaporation is dominant. Notice that dominant heat transfer mechanism determined by the corresponding $(h_{nb}/h_{cb})_{avg}$ value is generally in good agreement with that suggested by the original author(s) in Table 2 (*e.g.*, nucleate boiling dominance indicated by Bao et al. [29] correspond to $(h_{nb}/h_{cb})_{avg} = 5.24$, and convective boiling dominance indicated by Qu and Mudawar [26] correspond to $(h_{nb}/h_{cb})_{avg} = 0.26$). Interestingly, the Lazarek and Black [67] correlation, which is based on nucleate boiling dominant data for R113, shows good predictions for some nucleate boiling dominant data for refrigerants, but poor predictions for most convective boiling data. The Liu and Winterton [66] correlation, which is based on data corresponding to $D = 2.95–32.0$ mm, provides inferior predictions for most data corresponding to diameters below 2 mm. Additional details concerning the effects of channel hydraulic diameter, working fluid, and dominant heat transfer regime will be discussed below. The present correlation provides very good predictions for all individual databases, with the best overall MAE of 20.3% and with 23 databases predicted more accurately than any of the select previous correlations.

The accuracy and limitations of previous correlations are also assessed by comparing predictions over the entire range of hydraulic diameters as shown in Fig. 6. Among the select previous correlations, only those of Lazarek and Black [67] and Liu and Winterton

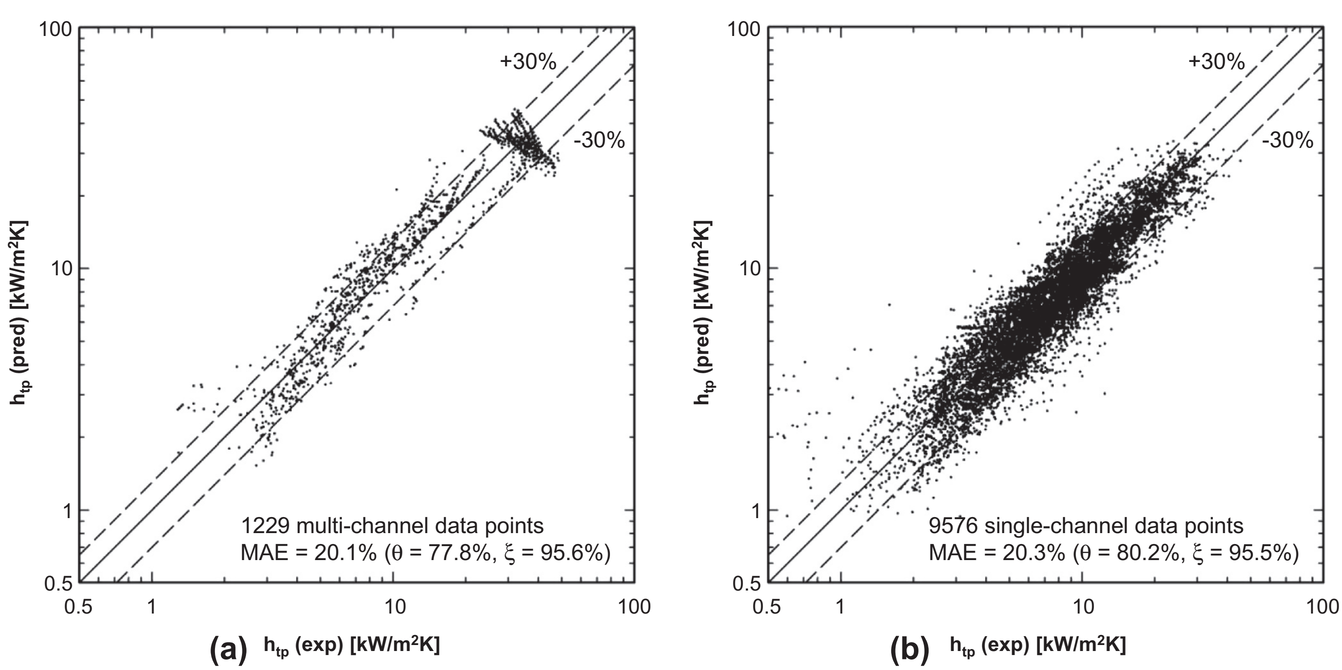

Fig. 8. Comparison of predictions of new correlation with two subsets of 10,805 point pre-dryout database corresponding to: (a) multi-channels and (b) single-channels.

[66] show relative good predictions for the range of 2.0–5.0 mm, with MAEs smaller than 25% for most bins. Notice, however, that the predictions of Lazarek and Black [67], Shah [63], and Liu and Winterton [66] are especially poor for very small diameters below 0.5 mm. In contrast, the predictive accuracy of the new correlation is fairly even over the entire range of diameters.

To further explore the accuracy of the present correlation, the effects of different working fluids are examined. Table 6 shows predictions of the present and select previous correlations compared to four subsets of the 10,805 point pre-dryout database: refrigerants, water, CO_2, and FC72. The results are also represented graphically in Fig. 7a–e for water, CO_2 and FC72. Excepting FC72 predictions by Lazarek and Black [67], the previous correlations are incapable of providing evenly good predictions for all four data subsets. The new correlation shows excellent predictions for all data subsets, evidenced by MAEs of 21.0% for refrigerants, 21.2% for water, 16.3% for CO_2, and 21.9% for FC72.

Table 7 shows predictions of the present and previous correlations with two subsets of the 10,805 point pre-dryout database: nucleate boiling dominant data and convective boiling dominant data. For the 8264 nucleate boiling dominant data, the correlations of Lazarek and Black [67] and Liu and Winterton [66] show relatively fair predictions, while, for the 2541 convective dominant data, predictions by all previous correlations are relatively poor. The new correlation provides the best predictions for both subsets, with MAEs of 20.7% and 19.0% for nucleate boiling dominant data and convective boiling dominant data, respectively.

Fig. 8a and b compare predictions of the new correlation with two subsets of the 10,805 point pre-dryout database corresponding to multi-channel flow and flow in single channels, respectively. The MAE for the 1229 multi-channel data subset is 20.1%, with 77.8% and 95.6% of the data falling within ±30% and ±50% error bands, respectively. The corresponding values for the 9576 single-channel data subset are MAE of 20.3%, and 80.2% and 95.5%

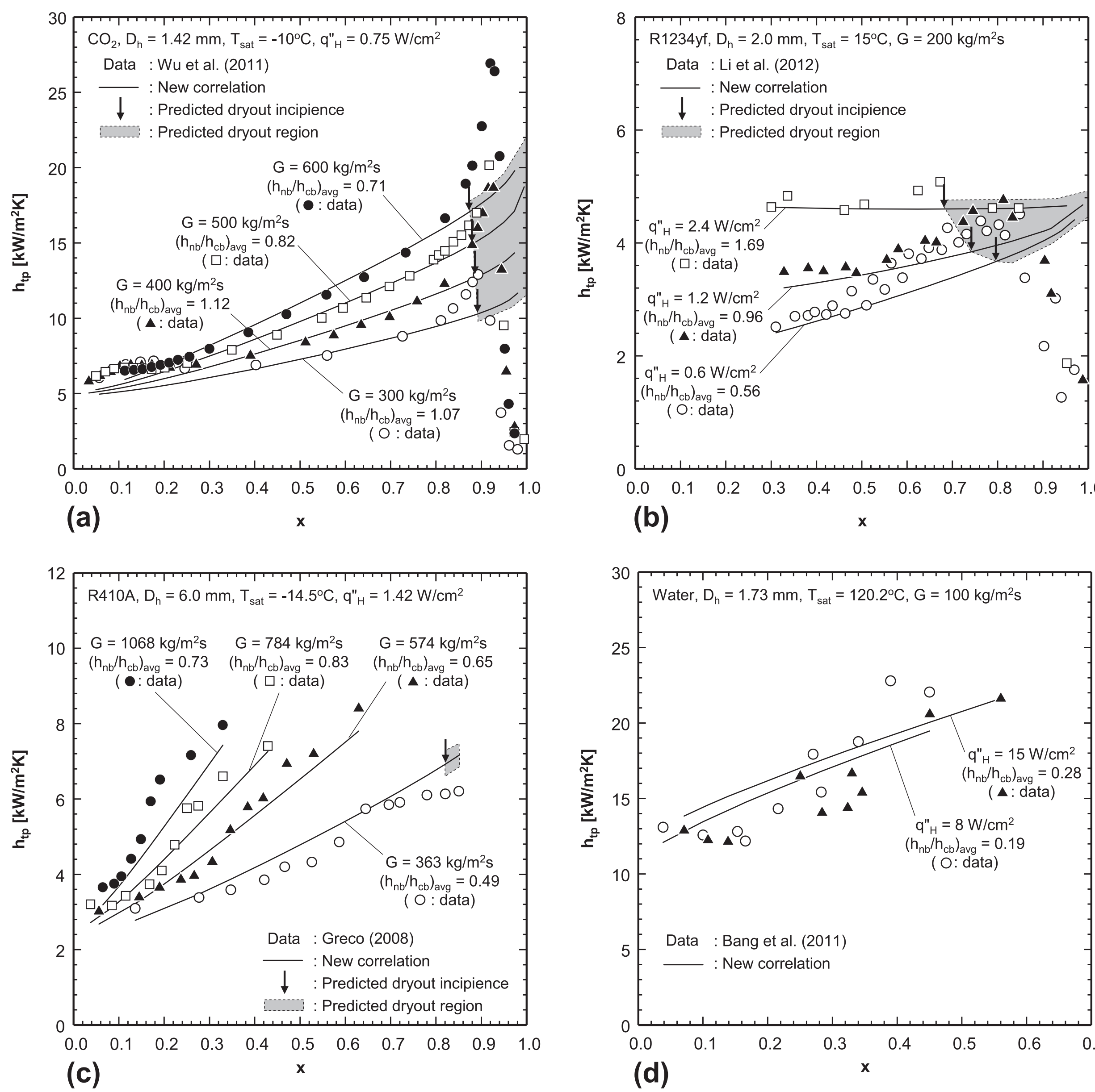

Fig. 9. Comparison of predictions of present heat transfer correlation with experimental data corresponding to convective boiling dominant heat transfer by: (a) Wu et al. [59], (b) Li et al. [61], (c) Greco [44], and (d) Bang et al. [28]. The case of $(h_{nb}/h_{cb})_{avg}$ = 1.69 in Fig. 9(b) is shown to illustrate the transition from convective boiling dominant to nucleate boiling dominant heat transfer.

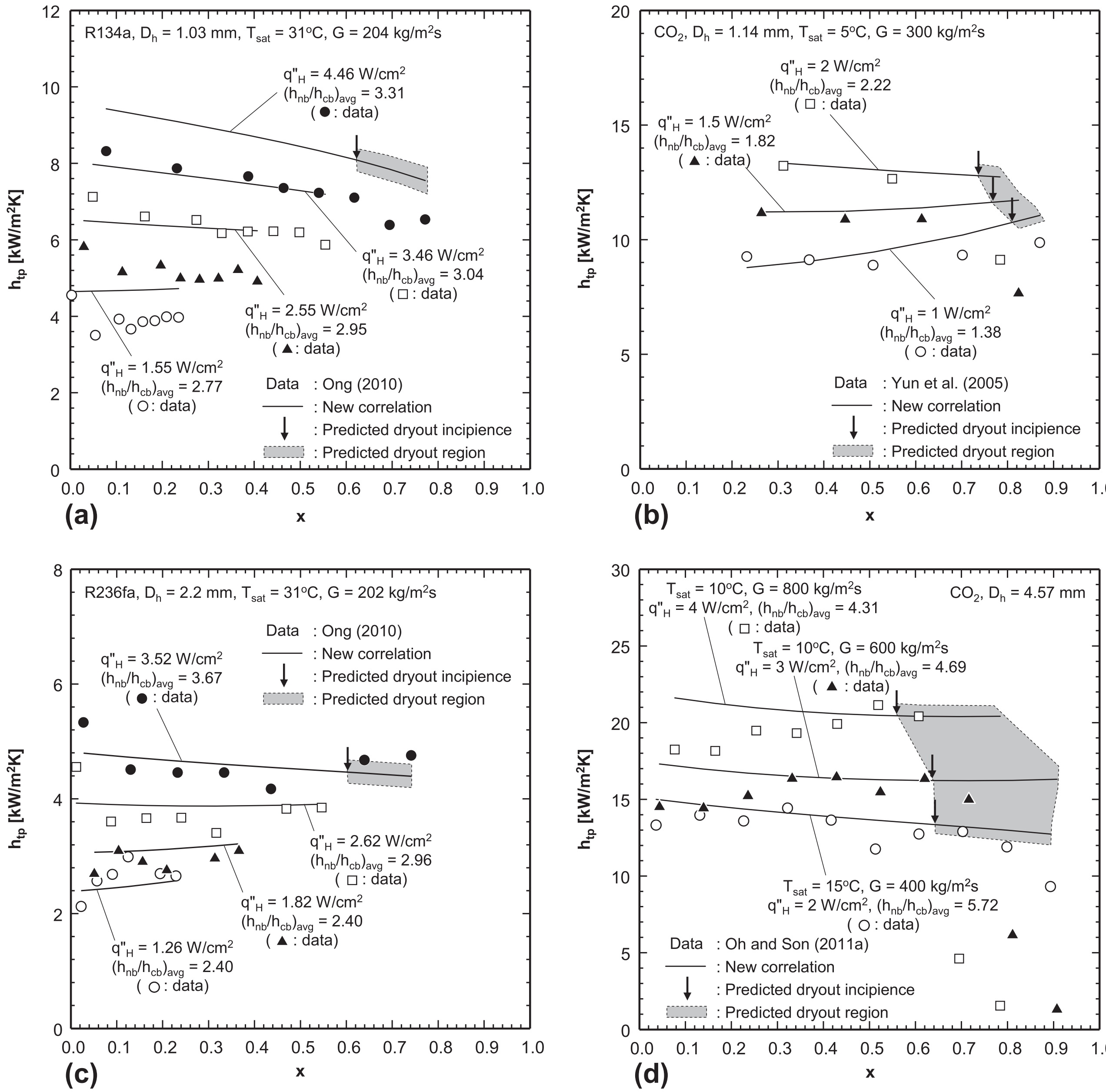

Fig. 10. Comparison of predictions of present heat transfer correlation with experimental data corresponding to nucleate boiling dominant heat transfer by: (a) Ong [53], (b) Yun et al. [39], (c) Ong [53], and (d) Oh and Son [31].

of the data falling within ±30% and ±50% error bands, respectively. This proves that the predictive capability of the new correlation is not compromised for specific subsets of the database.

To further examine the predictive accuracy of the new heat transfer correlation, its predictions are compared with representative convective boiling dominant data [28,44,61,59] and nucleate boiling dominant data [31,39,53], as shown in Figs. 9 and 10, respectively. These two figures also confirm the predictive accuracy of the dryout incipience quality correlation presented in the first part of this study [25] by identifying locations of dryout incipience corresponding to sudden decline in the heat transfer coefficient quite accurately. Notice that for $(h_{nb}/h_{cb})_{avg} < 1$, convective boiling is more dominant and h_{tp} has a positive slope vesus x, whereas nucleate boiling is dominant for $(h_{nb}/h_{cb})_{avg} > 1$, where h_{nb} and h_{cb} are calculated using the present correlation summarized in Table 4, and $(h_{nb}/h_{cb})_{avg}$ is averaged up to the location of dryout incipience.

For the convective boiling dominant regime, the heat transfer coefficient generally increases with increasing mass velocity in both the data and predictions, Fig. 9a and c, but is less sensitive to heat flux variations as shown in Fig. 9(d). However, as the contribution of nucleate boiling increases, as shown for $(h_{nb}/h_{cb})_{avg} = 1.69$ in Fig. 9(b), both the slope of h_{tp} versus x decreases and h_{tp} becomes sensitive to the increase in heat flux.

For the nucleate boiling dominant regime corresponding to high $(h_{nb}/h_{cb})_{avg}$ values, h_{tp} is sensitive to heat flux variations as shown in Fig. 10a–c, and the slope of h_{tp} versus x becomes negative with increasing heat flux, Fig. 10a–d. Figs. 9 and 10 prove that the new correlation accurately captures experimental data in both magnitude and trend.

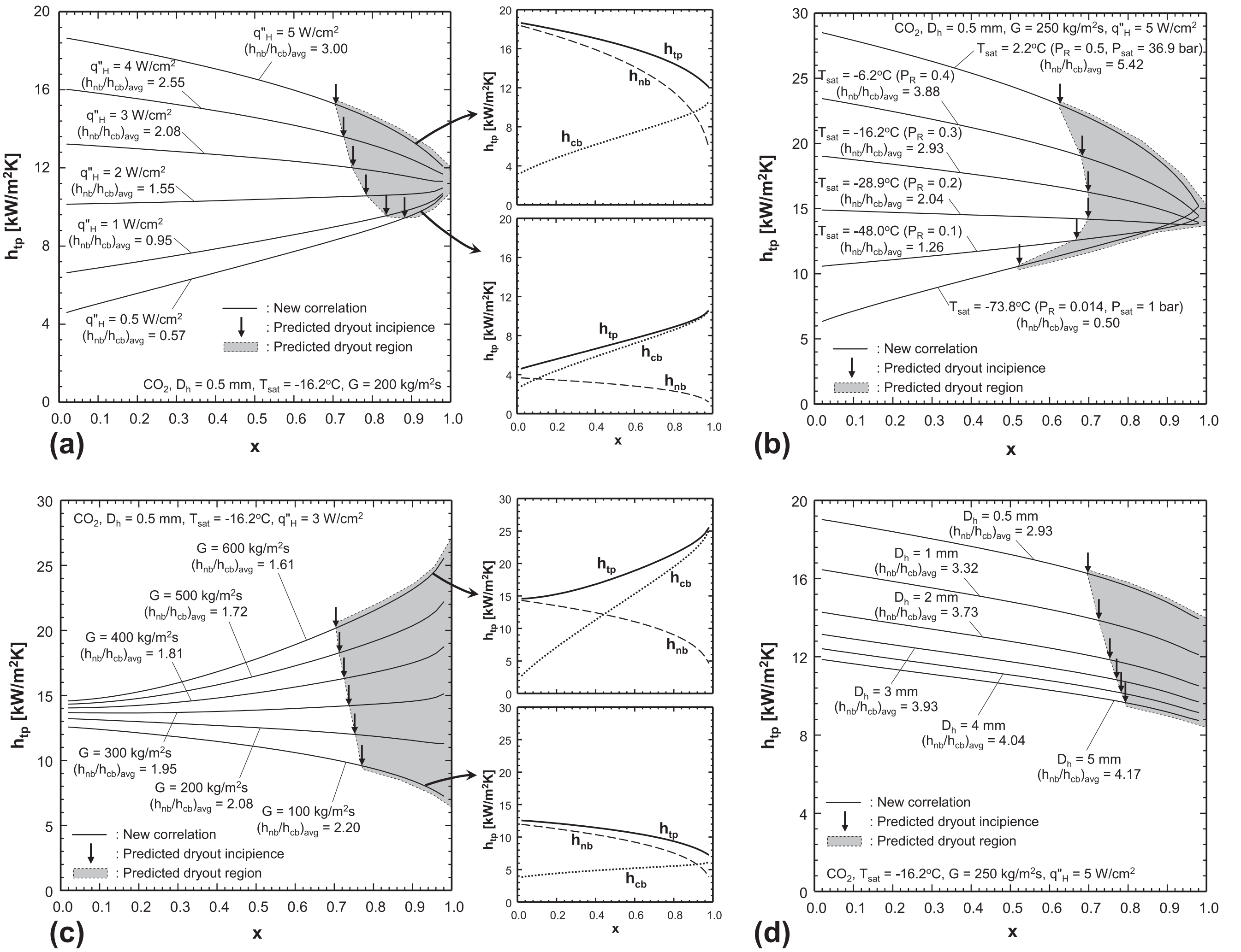

Fig. 11. Predicted effects of (a) heat flux, (b) saturation temperature, (c) mass velocity, and (d) channel diameter on the variation of two-phase heat transfer coefficient with quality.

Fig. 11a–d shows parametric trends of h_{tp} versus x corresponding to variations in heat flux, q''_H, saturation temperature, T_{sat}, mass velocity, G, and channel diameter, D_h, predicted by the new heat transfer correlation. Fig. 11(a) shows h_{tp} increases with increasing, q''_H because of the increasing contribution of nucleate boiling. Notice that the trend of h_{tp} versus x changes depending on the dominant heat transfer regime as shown in the two small plots in Fig. 11(a) corresponding to the highest and lowest q''_H values. h_{tp} decreases with increasing x where nucleate boiling is dominant (*i.e.*, $(h_{nb}/h_{cb})_{avg} \geqslant 1$), and increases with increasing x where convective boiling is dominant (*i.e.*, $(h_{nb}/h_{cb})_{avg} \leqslant 1$). Fig. 11(b) shows h_{tp} versus x for CO_2, with T_{sat} increasing from -73.8 to 2.2 °C, corresponding to an increase in reduced pressures from $P_R = 0.014$ to 0.5. The predicted heat transfer coefficient increases due to the dependence on P_R in Eq. (8b). The contribution of nucleate boiling increases with increasing T_{sat}, evidenced by increasing values of $(h_{nb}/h_{cb})_{avg}$, resulting in the slope of h_{tp} versus x changing from positive to negative. Fig. 11(c) shows h_{tp} increases with increasing G because of the increased contribution of convective boiling, which is mainly due to the increase in Re_f in the Dittus-Boelter relation in Eq. (8b). As shown in Fig. 11(d), increasing D_h decreases h_{tp} because of a decrease in h_{nb}. Here, $(h_{nb}/h_{cb})_{avg}$ increases with increasing D_h because h_{cb} decreases more rapidly than h_{nb}.

Fig. 12a–d shows parametric trends of h_{tp} versus x predicted by the new heat transfer correlation for water, CO_2, R134a, and FC72, respectively. The cases examined here are for a constant saturation pressure of $P_{sat} = 1$ bar, mass velocity of $G = 150$ kg/m^2 s, heat flux of $q''_H = 10$ W/cm^2, and hydraulic diameter of $D_h = 0.5$ mm. As shown in Fig. 12(a) for water, convective boiling is very dominant and nucleate boiling virtually nonexistent, resulting in h_{tp} increasing with increasing x. On the other hand, Fig. 12(d) shows for FC72 that nucleate boiling is dominant and h_{tp} decreases with increasing x. Relatively strong contribution of h_{cb} is observed for CO_2, Fig. 12(b), and of h_{nb} for R134a, Fig. 12(c), before the location of dryout incipience. Notice for R134a, how superimposing a decreasing h_{nb} with increasing h_{cb} causes h_{tp} to remain nearly constant with increasing x.

5. Conclusions

This paper is the second part of a two-part study addressing the prediction of heat transfer for saturated flow boiling in mini/micro-channels. The first part examined the determination of dryout incipience quality, which marks the location where the heat transfer coefficient begins to decrease appreciably. This part explored

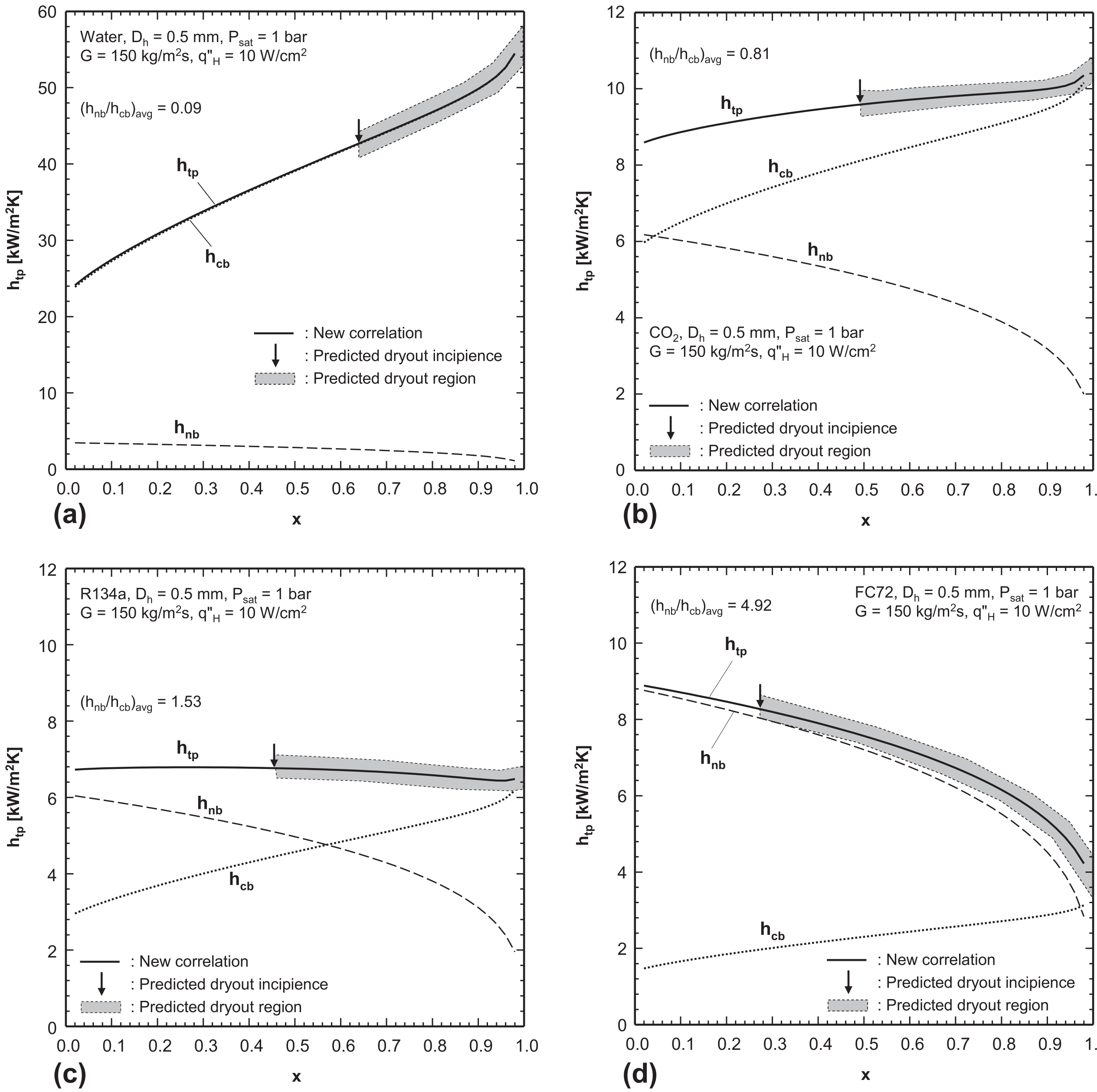

Fig. 12. Predicted variations of two-phase heat transfer coefficient variation with quality for (a) water, (b) CO_2, (c) R134a, and (d) FC72.

the development of a universal correlation for the pre-dryout two-phase heat transfer coefficient. Key findings from the study are as follows:

(1) A new consolidated database for flow boiling heat transfer in mini/micro-channels that consists of 12,974 data points was amassed from 31 sources. Of these, 10,805 are designated as pre-dryout data by using the correlation derived in the first part of this study. The pre-dryout database consists of 18 working fluids, hydraulic diameters of 0.19–6.5 mm, mass velocities of 19–1608 kg/m^2 s, liquid-only Reynolds numbers of 57–49,820, qualities of 0–1, and reduced pressures from 0.005 to 0.69. The database includes single- and multi-port data, and both uniform circumferential heating and rectangular channels with three-sided heating.

(2) The pre-dryout consolidated database was compared to previous correlations recommended for both macro-channels and mini/micro-channels. While a few of these correlations showed some success relative to others, none provided good predictive accuracy for all fluid categories. Additionally, some of the more successful correlations showed poor accuracy against high pressure and very small diameter data.

(3) A new generalized correlation is proposed, which is based on superpositioning the contributions of nucleate boiling and convective boiling. This correlation shows very good predictive accuracy against the entire pre-dryout database, evidenced by an overall MAE of 20.3%. The new correlation is also shown to provide evenly good predictions for all working fluids and all ranges of the database parameters, as well as both single- and multi-port data.

Acknowledgement

The authors are grateful for the partial support for this project from the National Aeronautics and Space Administration (NASA) under grant no. NNX13AC83G.

References

[1] T.C. Willingham, I. Mudawar, Forced-convection boiling and critical heat flux from a linear array of discrete heat sources, Int. J. Heat Mass Transfer 35 (1992) 2879–2890.

[2] T.N. Tran, M.W. Wambsganss, D.M. France, Small circular- and rectangular-channel boiling with two refrigerants, Int. J. Multiphase Flow 22 (1996) 485–498.

[3] H.J. Lee, S.Y. Lee, Heat transfer correlation for boiling flows in small rectangular horizontal channels with low aspect ratios, Int. J. Multiphase Flow 27 (2001) 2043–2062.

[4] T.M. Anderson, I. Mudawar, Microelectronic cooling by enhanced pool boiling of a dielectric fluorocarbon liquid, J. Heat Transfer Trans. ASME 111 (1989) 752–759.

[5] I. Mudawar, A.H. Howard, C.O. Gersey, An analytical model for near-saturated pool boiling CHF on vertical surfaces, Int. J. Heat Mass Transfer 40 (1997) 2327–2339.

[6] Y. Katto, M. Kunihiro, Study of the mechanism of burn-out in boiling system of high burn-out heat flux, Bull. JSME 16 (1973) 1357–1366.

[7] M. Monde, T. Inoue, Critical heat flux in saturated forced convective boiling on a heated disk with multiple impinging jets, J. Heat Transfer Trans. ASME 113 (1991) 722–727.

[8] D.C. Wadsworth, I. Mudawar, Enhancement of single-phase heat transfer and critical heat flux from an ultra-high-flux-source to a rectangular impinging jet of dielectric liquid, J. Heat Transfer Trans. ASME 114 (1992) 764–768.

[9] M.E. Johns, I. Mudawar, An ultra-high power two-phase jet-impingement avionic clamshell module, J. Electron. Packag. Trans. ASME 118 (1996) 264–270.

[10] S. Toda, A study in mist cooling (1st report: investigation of mist cooling), Trans. JSME 38 (1972) (1972) 581–588.

[11] L. Lin, R. Ponnappan, Heat transfer characteristics of spray cooling in a closed loop, Int. J. Heat Mass Transfer 46 (2003) 3737–3746.

[12] J.R. Rybicki, I. Mudawar, Single-phase and two-phase cooling characteristics of upward-facing and downward-facing sprays, Int. J. Heat Mass Transfer 49 (2006) 5–16.

[13] M. Visaria, I. Mudawar, Theoretical and experimental study of the effects of spray orientation on two-phase spray cooling and critical heat flux, Int. J. Heat Mass Transfer 51 (2008) 2398–2410.

[14] W. Nakayama, T. Nakajima, S. Hirasawa, Heat sink studs having enhanced boiling surfaces for cooling of microelectronic components, ASME Paper 84-WA/HT-89, 1984.

[15] R.L. Webb, The evolution of enhanced surface geometries for nucleate boiling, Heat Transfer Eng. 2 (1981) 46–69.

[16] V. Khanikar, I. Mudawar, T. Fisher, Effects of carbon nanotube coating on flow boiling in a micro-channel, Int. J. Heat Mass Transfer 52 (2009) 3805–3817.

[17] M.K. Sung, I. Mudawar, Experimental and numerical investigation of single-phase heat transfer using a hybrid jet-impingement/micro-channel cooling scheme, Int. J. Heat Mass Transfer 49 (2006) 682–694.

[18] M.K. Sung, I. Mudawar, Correlation of critical heat flux in hybrid jet impingement/micro-channel cooling scheme, Int. J. Heat Mass Transfer 49 (2006) 2663–2672.

[19] D.D. Hall, I. Mudawar, Ultra-high critical heat flux (CHF) for subcooled water flow boiling–II. High-CHF database and design parameters, Int. J. Heat Mass Transfer 42 (1999) 1429–1456.

[20] D.D. Hall, I. Mudawar, Critical heat flux (CHF) for water flow in tubes–I. Compilation and assessment of world CHF data, Int. J. Heat Mass Transfer 43 (2000) 2573–2604.

[21] D.D. Hall, I. Mudawar, Critical heat flux (CHF) for water flow in tubes–II. Subcooled CHF correlations, Int. J. Heat Mass Transfer 43 (2000) 2605–2640.

[22] S.M. Kim, I. Mudawar, Universal approach to predicting two-phase frictional pressure drop for adiabatic and condensing mini/micro-channel flows, Int. J. Heat Mass Transfer 55 (2012) 3246–3261.

[23] S.M. Kim, I. Mudawar, Universal approach to predicting two-phase frictional pressure drop for mini/micro-channel saturated flow boiling, Int. J. Heat Mass Transfer 58 (2013) 718–734.

[24] S.M. Kim, I. Mudawar, Universal approach to predicting heat transfer coefficient for condensing mini/micro-channel flows, Int. J. Heat Mass Transfer 56 (2013) 238–250.

[25] S.M. Kim, I. Mudawar, Universal approach to predicting saturated flow boiling heat transfer in mini/micro-channels – Part I. Dryout incipience quality, Int. J. Heat Mass Transfer, (2013), http://dx.doi.org/10.1016/j.ijheatmasstransfer.2013.04.016.

[26] W. Qu, I. Mudawar, Flow boiling heat transfer in two-phase micro-channel heat sinks-I. Experimental investigation and assessment of correlation methods, Int. J. Heat Mass Transfer 46 (2003) 2755–2771.

[27] B. Sumith, F. Kaminaga, K. Matsumura, Saturated flow boiling of water in a vertical small diameter tube, Exp. Therm. Fluid Sci. 27 (2003) 789–801.

[28] K.H. Bang, K.K. Kim, S.K. Lee, B.W. Lee, Pressure effect on flow boiling heat transfer of water in minichannels, Int. J. Therm. Sci. 50 (2011) 280–286.

[29] Z.Y. Bao, D.F. Fletcher, B.S. Haynes, Flow boiling heat transfer of Freon R11 and HCFC123 in narrow passages, Int. J. Heat Mass Transfer 43 (2000) 3347–3358.

[30] X. Huo, L. Chen, Y.S. Tian, T.G. Karayiannis, Flow boiling and flow regimes in small diameter tubes, Appl. Therm. Eng. 24 (2004) 1225–1239.

[31] H.K. Oh, C.H. Son, Flow boiling heat transfer and pressure drop characteristics of CO_2 in horizontal tube of 4.57-mm inner diameter, Appl. Therm. Eng. 31 (2011) 163–172.

[32] M.W. Wambsganss, D.M. France, J.A. Jendrzejczyk, T.N. Tran, Boiling heat transfer in a horizontal small-diameter tube, ASME J. Heat Transfer 115 (1993) 963–972.

[33] T.N. Tran, Pressure drop and heat transfer study of two-phase flow in small channels, Ph.D. Thesis, Texas Tech University, TX, 1998.

[34] C.C. Wang, C.S. Chiang, J.G. Yu, An experimental study of in-tube evaporation of R-22 inside a 6.5-mm smooth tube, Int. J. Heat Fluid Flow 19 (1998) 259–269.

[35] Y.Y. Yan, T.F. Lin, Evaporation heat transfer and pressure drop of refrigerant R-134a in a small pipe, Int. J. Heat Mass Transfer 41 (1998) 4183–4194.

[36] R. Yun, Y. Kim, M.S. Kim, Y. Choi, Boiling heat transfer and dryout phenomenon of CO_2 in a horizontal smooth tube, Int. J. Heat Mass Transfer 46 (2003) 2353–2361.

[37] J. Lee, I. Mudawar, Two-phase flow in high-heat-flux micro-channel heat sink for refrigeration cooling applications: Part II–heat transfer characteristics, Int. J. Heat Mass Transfer 48 (2005) 941–955.

[38] S. Saitoh, H. Daiguji, E. Hihara, Effect of tube diameter on boiling heat transfer of R-134a in horizontal small-diameter tubes, Int. J. Heat Mass Transfer 48 (2005) 4973–4984.

[39] R. Yun, Y. Kim, M.S. Kim, Convective boiling heat transfer characteristics of CO_2 in microchannels, Int. J. Heat Mass Transfer 48 (2005) 235–242.

[40] R. Muwanga, I. Hassan, A flow boiling heat transfer investigation of FC-72 in a microtube using liquid crystal thermography, ASME J. Heat Transfer 129 (2007) 977–987.

[41] X. Zhao, P.K. Bansal, Flow boiling heat transfer characteristics of CO_2 at low temperatures, Int. J. Refrig. 30 (2007) 937–945.

[42] B. Agostini, J.R. Thome, M. Fabbri, B. Michel, D. Calmi, U. Kloter, High heat flux flow boiling in silicon multi-microchannels – Part I: heat transfer characteristics of refrigerant R236fa, Int. J. Heat Mass Transfer 51 (2008) 5400–5414.

[43] L. Consolini, Convective boiling heat transfer in a single micro-channel, Ph.D. Thesis, École Polytechnique Fédérale De Lausanne, Switzerland, 2008.

[44] A. Greco, Convective boiling of pure and mixed refrigerants: an experimental study of the major parameters affecting heat transfer, Int. J. Heat Mass Transfer 51 (2008) 896–909.

[45] S.S. Bertsch, E.A. Groll, S.V. Garimella, Effects of heat flux, mass flux, vapor quality, and saturation temperature on flow boiling heat transfer in microchannels, Int. J. Multiphase Flow 35 (2009) 142–154.

[46] S. In, S. Jeong, Flow boiling heat transfer characteristics of R123 and R134a in a micro-channel, Int. J. Multiphase Flow 35 (2009) 987–1000.

[47] R. Mastrullo, A.W. Mauro, A. Rosato, G.P. Vanoli, Carbon dioxide local heat transfer coefficients during flow boiling in a horizontal circular smooth tube, Int. J. Heat Mass Transfer 52 (2009) 4184–4194.

[48] H. Ohta, K. Inoue, M. Ando, K. Watanabe, Experimental investigation on observed scattering in heat transfer characteristics for flow boiling in a small diameter tube, Heat Transfer Eng. 30 (2009) 19–27.

[49] L. Wang, M. Chen, M. Groll, Flow boiling heat transfer characteristics of R134a in a horizontal mini tube, J. Chem. Eng. Data 54 (2009) 2638–2645.

[50] M. Ducoulombier, Ébullition convective du dioxyde de carbone – étude expérimentale en micro-canal, Ph.D. Thesis, Institut National des Sciences Appliquées (INSA) de Lyon, France, 2010.

[51] M. Hamdar, A. Zoughaib, D. Clodic, Flow boiling heat transfer and pressure drop of pure HFC-152a in a horizontal mini-channel, Int. J. Refrig. 33 (2010) 566–577.

[52] C. Martín-Callizo, Flow boiling heat transfer in single vertical channel of small diameter, Ph.D. Thesis, Royal Institute of Technology, Sweden, 2010.

[53] C.L. Ong, Macro-to-microchannel transition in two-phase flow and evaporation, Ph.D. Thesis, École Polytechnique Fédérale De Lausanne, Switzerland, 2010.

[54] C.B. Tibiriçá, G. Ribatski, Flow boiling heat transfer of R134a and R245fa in a 2.3 mm tube, Int. J. Heat Mass Transfer 53 (2010) 2459–2468.

[55] R. Ali, B. Palm, M.H. Maqbool, Flow boiling heat transfer characteristics of a minichannel up to dryout condition, ASME J. Heat Transfer 133 (2011) 081501.

[56] J.B. Copetti, M.H. Macagnan, F. Zinani, N.L.F. Kunsler, Flow boiling heat transfer and pressure drop of R-134a in a mini tube: an experimental investigation, Exp. Therm. Fluid Sci. 35 (2011) 636–644.

[57] M.M. Mahmoud, T.G. Karayiannis, D.B.R. Kenning, Surface effects in flow boiling of R134a in microtubes, Int. J. Heat Mass Transfer 54 (2011) 3334–3346.

[58] H.K. Oh, C.H. Son, Evaporation flow pattern and heat transfer of R-22 and R-134a in small diameter tubes, Heat Mass Transfer 47 (2011) 703–717.

[59] J. Wu, T. Koettig, Ch. Franke, D. Helmer, T. Eisel, F. Haug, J. Bremer, Investigation of heat transfer and pressure drop of CO_2 two-phase flow in a horizontal minichannel, Int. J. Heat Mass Transfer 54 (2011) 2154–2162.

[60] T.G. Karayiannis, M.M. Mahmoud, D.B.R. Kenning, A study of discrepancies in flow boiling results in small to microdiameter metallic tubes, Exp. Therm. Fluid Sci. 36 (2012) 126–142.

[61] M. Li, C. Dang, E. Hihara, Flow boiling heat transfer of HFO1234yf and R32 refrigerant mixtures in a smooth horizontal tube: part I. Experimental investigation, Int. J. Heat Mass Transfer 55 (2012) 3437–3446.
[62] C.B. Tibiriçá, G. Ribatski, J.R. Thome, Flow boiling characteristics for R1234ze(E) in 1.0 and 2.2 mm circular channels, ASME J. Heat Transfer 134 (2012) 020906.
[63] M.M. Shah, Chart correlation for saturated boiling heat transfer: equations and further study, ASHRAE Trans. 88 (1982) 185–196.
[64] M.G. Cooper, Saturation nucleate pool boiling – a simple correlation, I. Chem. Eng. Symp. Ser. 86 (1984) 785–793.
[65] K.E. Gungor, R.H.S. Winterton, A general correlation for flow boiling in tubes and annuli, Int. J. Heat Mass Transfer 29 (1986) 351–358.
[66] Z. Liu, R.H.S. Winterton, A general correlation for saturated and subcooled flow boiling in tubes and annuli, based on a nucleate pool boiling equation, Int. J. Heat Mass Transfer 34 (1991) 2759–2766.
[67] G.M. Lazarek, S.H. Black, Evaporative heat transfer, pressure drop and critical heat flux in a small vertical tube with R-113, Int. J. Heat Mass Transfer 25 (1982) 945–960.
[68] T.N. Tran, M.W. Wambsganss, D.M. France, Small circular- and rectangular-channel boiling with two refrigerants, Int. J. Multiphase Flow 22 (1996) 485–498.
[69] G.R. Warrier, V.K. Dhir, L.A. Momoda, Heat transfer and pressure drop in narrow rectangular channels, Exp. Therm. Fluid Sci. 26 (2002) 53–64.
[70] W. Yu, D.M. France, M.W. Wambsganss, J.R. Hull, Two-phase pressure drop, boiling heat transfer, and critical heat flux to water in a small-diameter horizontal tube, Int. J. Multiphase Flow 28 (2002) 927–941.
[71] B. Agostini, A. Bontemps, Vertical flow boiling of refrigerant R134a in small channels, Int. J. Heat Fluid Flow 26 (2005) 296–306.
[72] S.S. Bertsch, E.A. Groll, S.V. Garimella, A composite heat transfer correlation for saturated flow boiling in small channels, Int. J. Heat Mass Transfer 52 (2009) 2110–2118.
[73] W. Li, Z. Wu, A general correlation for evaporative heat transfer in micro/mini-channels, Int. J. Heat Mass Transfer 53 (2010) 1778–1787.
[74] M. Ducoulombier, S. Colasson, J. Bonjour, P. Haberschill, Carbon dioxide flow boiling in a single microchannel – part II: heat transfer, Exp. Therm. Fluid Sci. 35 (2011) 597–611.
[75] E.W. Lemmon, M.L. Huber, M.O. McLinden, Reference fluid thermodynamic and transport properties – REFPROP Version 8.0, NIST, MD, 2007.
[76] S.M. Kim, I. Mudawar, Flow condensation in parallel micro-channels – part 2: heat transfer results and correlation technique, Int. J. Heat Mass Transfer 55 (2012) 984–994.
[77] R.K. Shah, A.L. London, Laminar Flow Forced Convection in Ducts: a source Book for Compact Heat Exchanger Analytical Data, Academic press, New York, 1978. Suppl. 1.
[78] V.E. Schrock, L.M. Grossman, Forced convection boiling in tubes, Nucl. Sci. Eng. 12 (1962) 474–481.
[79] R.W. Lockhart, R.C. Martinelli, Proposed correlation of data for isothermal two-phase, two-component flow in pipes, Chem. Eng. Prog. 45 (1949) 39–48.
[80] S.W. Churchill, R. Usagi, A general expression for the correlation of rates of transfer and other phenomena, AIChE J. 18 (1972) 1121–1128.